α-Synuclein Fibril Formation and the Effects of Lipid Membranes

Gaspar, Ricardo

2018

Document Version:
Publisher's PDF, also known as Version of record

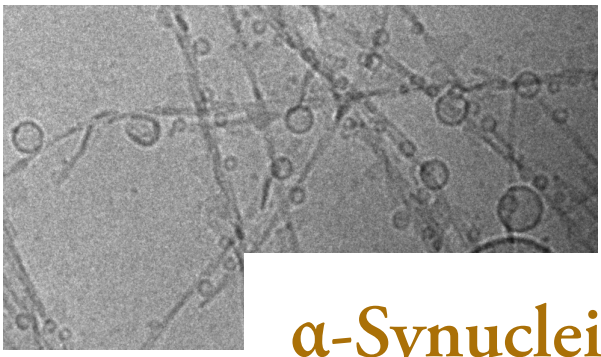
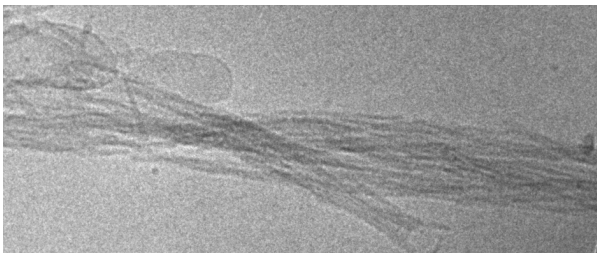

α-Synuclein Fibril Formation and the Effects of Lipid Membranes

RICARDO GASPAR | PHYSICAL CHEMISTRY | LUND UNIVERSITY


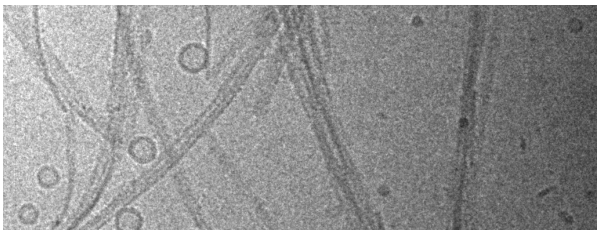
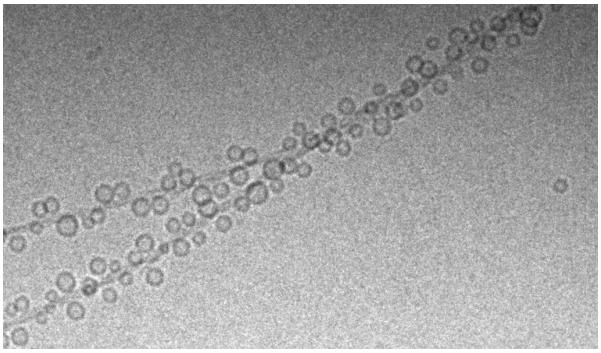
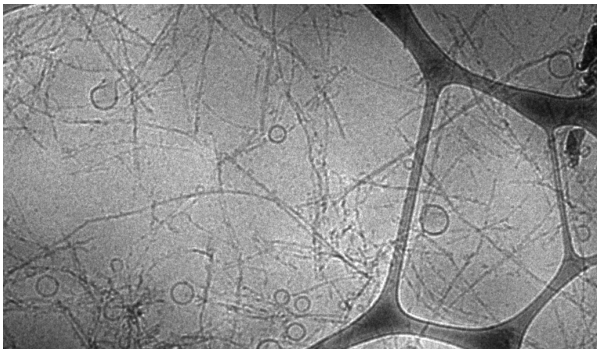
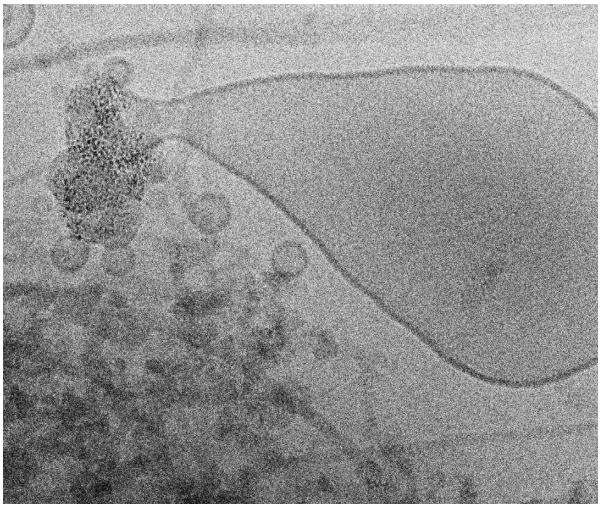


α-Synuclein Fibril Formation and the Effects of Lipid Membranes

Ricardo Lourenço Gaspar

LUND
UNIVERSITY

DOCTORAL DISSERTATION
by due permission of the Faculty of Science, Lund University, Sweden.
To be defended on Friday, the 26th of October 2018 at 9:00 in lecture Hall C, Kemicentrum, Lund University.

Faculty opponent
Prof. Dr. Roland Riek, Laboratory of Physical-Chemistry, Department of Chemistry and Applied Biosciences, ETH Zurich, Switzerland

Organization	Document name
LUND UNIVERSITY PO BOX 124 SE-22100 Lund, Sweden	DOCTORAL DISSERTATION
	Date of issue 2018-10-02
Author(s) Ricardo Lourenço Gaspar	Sponsoring organization

Title and subtitle

α-Synuclein Fibril Formation and the Effects of Lipid Membranes

Abstract

Amyloid protein aggregation results in major disturbances of cellular processes in humans. The most common amyloid-related disorders are Alzheimer´s disease and Parkinson´s disease. Parkinson´s disease is charaterized by the formation of protein-rich aggregates that are deposited in neurons, termed Lewy bodies and Lewy neurites. The main component identified in these protein-rich deposits is the peptide α-synuclein.

The work described here is mainly focused on *in vitro* aggregation studies of α-synuclein alone and in the presence of lipid membranes of different compositions. This is possible as we have identified conditions leading to reproducible thioflavin-T aggregation kinetics. The aggregation mechanism of α-synuclein was shown to be pH dependent. At neutral pH, both homogeneous primary nucleation and secondary processes are undetectable. At mildly acidic pH, present in the lumens of some intracellular compartments, secondary processes are enhanced. Experiments were performed to identify the nature of these secondary processes, distinguishing between fragmentation of fibrils and nucleation of monomers on the surface of existing aggregates. It was found that monomer-dependent secondary nucleation is the underlying dominant microscopic event of the aggregation process at mildly acidic pH, providing an autocatalytic amyloid amplification event. Crystallin chaperones purified from bovine eye lens were shown capable of inhibiting fibril formation of α-synuclein by affecting both secondary nucleation and elongation processes.

In amyloid plaques associated with several amyloidogenic diseases, tightly associated lipids have been identified. We explore how lipid membranes interfere with the aggregation mechanism of α-synuclein. Our results show a dependence of the aggregation rate on lipid composition and lipid charge. Biological exosomes, isolated from neuroblastoma cells, were shown to accelerate α-synuclein aggregation. This effect was found to be due to neuro-specific ganglioside lipids. Investigating the catalytic effect of anionic lipid membranes on α-synuclein aggregation, it was shown that charge-based interactions, induce conformational change of α-synuclein from random coil to α-helix, and is also associated with rapid aggregation kinetics. However, charge-independent interactions are also important, as lipid membranes containing uncharged lipid species with large hydrophilic headgroups were shown capable of triggering α-synuclein aggregation, although far less efficiently and without inducing α-synuclein conformational change to α-helix.

Investigating α-synuclein-ganglioside co-aggregation by imaging with cryo-EM at different time points along the aggregation reaction revealed aggregates with different structural morphology compared to those formed from pure α-synuclein. The images show a clear evolution of the vesicle size distribution, with a dramatic decrease in vesicle size during the lagphase of the aggregation reaction. Co-aggregates are thin and curly, decorated with small and monodisperse lipid vesicles contrary to compact bundles observed for fibrils formed from protein alone.

Key words

Protein misfolding, α-synuclein, Parkinson´s disease, microscopic rate constants, thioflavin-T, ganglioside lipids, exosomes, protein-lipid co-aggregation, model membranes, monomer-dependent secondary nucleation

Classification system and/or index terms (if any)

Supplementary bibliographical information		Language English
ISSN and key title		ISBN 978-91-7422-599-0 (printed) 978-91-7422-600-3 (digital)
Recipient's notes	Number of pages 254	Price
	Security classification	

α-Synuclein Fibril Formation and the Effects of Lipid Membranes

Ricardo Lourenço Gaspar

LUND
UNIVERSITY

Front Cover: Cryo-TEM images of aggregating α-synuclein in the presence of 9:1 DOPC/GM1 lipid vesicles taken at different time points along the aggregation reaction.

Back Cover: Cryo-TEM image taken by Marie Grey of aggregating α-synuclein in the presence of exosomes after 68h incubation time. Every time I think about my time in Sweden and my PhD, my face makes a similar expression…

Supervisors: Professor Emma Sparr

Professor Sara Linse

α-Synuclein Fibril Formation and the Effects of Lipid Membranes

Division of Physical Chemistry
Division of Biochemistry and Structural Biology
Department of Chemistry
Lund University

ISBN 978-91-7422-599-0 (printed)
ISBN 978-91-7422-600-3 (digital)

Printed in Sweden by Media-Tryck, Lund University
Lund 2018

Media-Tryck is an environmentally certified and ISO 14001 certified provider of printed material. Read more about our environmental work at www.mediatryck.lu.se

In loving memory of David Lourenço Gaspar

"Upon my
Heart I Wear
a Frown"

Preface

The deposition of protein-rich aggregates termed Lewy bodies and Lewy neurites and the spreading of the pathology throughout the brain are hallmarks of Parkinson´s disease. The main component found in such protein inclusions is α-synuclein. The aggregation mechanism of α-synuclein was found to be pH dependent (paper I,II and VII). At neutral pH (Paper I), homogeneous primary nucleation and secondary processes, such as fragmentation of fibrils and nucleation of monomers on the surface of existing aggregates, are undetectable. For mildly acidic pH (Paper I, II and VII), present in some lumens of intracellular compartments, the molecular mechanism underlying the aggregation process is dominated by monomer-dependent secondary nucleation. Secondary nucleation consists of a double threat, increasing rapidly both the load of fibrillar mass and the amount of smaller oligomeric species often linked to cytotoxicity. α-Synuclein fibril formation was shown to be inhibited by crystallin chaperone proteins, purified from bovine eye lens (Paper III). The inhibitory effect of crystallins was shown to be time-dependent, with early additions of crystallin capable of retarding aggregation, affecting both elongation and monomer-dependent secondary nucleation.

Amyloid protein interaction and co-aggregation with lipid membranes is of critical importance in biology, potentially associated with toxicity and propagation of Parkinson´s disease. Spectroscopy, microscopy, protein chemistry and surface techniques have been here used to address and investigate the influence of lipid membranes on the aggregation of α-synuclein, structure of co-aggregates, lipid composition and lipid dynamics in the co-aggregates (Paper IV – VII). The studies take advantage of well characterized and reproducible aggregation kinetics. It was demonstrated that monomeric α-synuclein readily associates with anionic lipid membranes at slightly acidic pH conditions due to electrostatic interactions (Paper VII). In membrane-induced aggregation, when the protein adsorbs to anionic lipid membranes, it induces α-synuclein conformational change from random coil to α-helix and accelerates the aggregation kinetics (Paper V). In particular, ganglioside lipids found in high amounts in neurons and exosomes, were shown to be more efficient in accelerating α-synuclein aggregation as compared to other anionic lipid systems (Paper IV and V). Interactions with uncharged lipid membranes are also relevant in membrane-induced aggregation although the catalytic effect was shown to be far less pronounced for all uncharged model systems investigated (Paper V).

The lipid-protein co-aggregates formed in systems containing gangliosides are shown to have distinct structure and morphology when compared to pure protein aggregates (Paper VI). Changes in surface properties of the amyloid aggregates due to the presence of lipids may also modulate the aggregation mechanism by interfering with surface-dependent processes like monomer-dependent secondary nucleation. Our results may provide novel insights by bridging fundamental understandings with the role of these aggregates in biological systems.

The described project on amyloid protein interactions with lipid membranes may add to the understanding of the molecular mechanisms behind Parkinson's disease. There are indications that protein-lipid co-aggregation is a physiologically important phenomenon, and if this is the case, the research will have impact on both medical practice and the scientific community.

List of Papers

I. **Solution conditions determine the relative importance of nucleation and growth processes in α-synuclein aggregation**
Alexander K. Buell, Céline Galvagnion, Ricardo Gaspar, Emma Sparr, Michele Vendruscolo, Tuomas P. J. Knowles, Sara Linse and Christopher M. Dobson
Proc. Natl. Acad. Sci. USA **2014**, 111(21): 7671-7676

II. **Secondary nucleation of monomers on fibril surface dominates α-synuclein aggregation and provides autocatalytic amyloid amplification**
Ricardo Gaspar, Georg Meisl, Alexander K. Buell, Laurence Young, Clemens F. Kaminski, Tuomas P. J. Knowles, Emma Sparr and Sara Linse
QRB-Discovery **2017**, 50(e6): 1-12

III. **Eye lens crystallin proteins inhibit α-synuclein fibril formation**
Ricardo Gaspar, Tommy Garting, Anna Stradner
Manuscript

IV. **Acceleration of α-synuclein aggregation by exosomes**
Marie Grey*, Christopher J. Dunning*, Ricardo Gaspar*, Patrik Brundin, Emma Sparr and Sara Linse (*authors contributed equally)
Journal of Biological Chemistry **2015**, 290(5): 2969-2982

V. **Ganglioside lipids accelerate α-synuclein amyloid formation**
Ricardo Gaspar, Jon Pallbo, Ulrich Weininger, Sara Linse and Emma Sparr
BBA- proteins and proteomics **2018**, 1866: 1062-1072.

VI. **Lipid-protein co-aggregation process monitored with cryo-TEM**

Ricardo Gaspar, Sara Linse and Emma Sparr

Manuscript

VII. **On the origin of anomalous salt dependence in α-synuclein fibril formation**

Ricardo Gaspar, Mikael Lund, Emma Sparr and Sara Linse

Manuscript

Not included in the thesis:

Acceleration of α-synuclein aggregation

Ricardo Gaspar, Georg Meisl, Alexander K. Buell, Laurence Young, Clemens F. Kaminski, Tuomas P. J. Knowles, Emma Sparr and Sara Linse

Amyloid **2017**, 24(S1): 20-21

Author Contributions

I. I, ES and SL designed the experiments at low pH; I performed the kinetic experiments from pH 5.5 to 6.5; I analyzed the data together with ES and SL; I contributed to the writing of the paper.

II. I, AKB, CK, TPJK, ES and SL designed the experiments; I performed all experiments except the QCM-D done by AKB; I and LY performed the dSTORM experiments; I analyzed the data together with GM and also TPJK, ES and SL; I wrote the first draft of the paper with input from ES, SL and also with contribution from all authors.

III. I designed the experiments; I performed all experiments except the purification of crystallin proteins done by TG and AS; I analyzed the data; I wrote the first draft of the paper with input from the co-authors, ES and SL.

IV. I and MG performed the kinetic experiments and cryo-TEM; I and MG analyzed the data together with ES, SL and all authors; I contributed to the writing of the paper.

V. I, ES and SL designed the study; I performed all the experiments; I and JP performed the CD experiments; I and UW performed the NMR experiments; I, JP, UW, SL and ES analyzed the data; I wrote the first draft of the paper with input from SL, ES and also with contribution from all authors.

VI. All authors designed the study. I performed the experiments; I wrote the first draft of the paper with input from SL and ES.

VII. All authors involved in the design of the study; I performed all experiments; I analyzed data together with ES and SL; I wrote the first draft of the paper with input from ML, ES and SL.

“I ain´t getting on no plane, fool!”
Sergeant B.A. Baracus from The A-Team

Table of Contents

List of abbreviations

IDP	Intrinsically disordered protein
PD	Parkinson´s disease
AD	Alzheimer´s disease
α-syn	α-synuclein
β-syn	β-synuclein
NAC	Non-amyloid-β component
Aβ	Amyloid-β
ThT	Thioflavin-T
SUV	Small unilamellar vesicles
CD	Circular Dichroism
QCM	Quartz Crystal Microbalance
SEC	Size-exclusion chromatography
dSTORM	Direct stochastic optical reconstruction microscopy
PEGylated plates	Non-binding plates coated with PEG
GM	Ganglioside lipids
PA	Phosphatidic acid
PI	Phosphatidylinositol
PE	Phosphoethanolamine
PS	Phosphatidylserine
CL	Cardiolipin

1.Introduction

1.1 Proteins: Building blocks of life - "A Protein Shake a Day Keeps the Doctor Away"

Proteins are elegantly folded macromolecules made up of small amino acid units, responsible for nearly all tasks of cellular life. Each protein typically folds into a specific structure that will lead to a specific function. In protein assemblies, the backbone of the molecular structure is quite similar, differing from one another in their side-chains. These side-chains consist of small molecular groups that are exposed to the environment and are specific for each amino acid (1). Multiple specific interactions between side-chains lead to a unique protein native fold. Protein folding is a spontaneous process on the short timescales striving towards minimal free energy. Commonly, polypeptides form α-helices and β-sheets as a result of the geometry of chemical bonds and the steric hindrance of atoms between side chains (1). Proteins that lack a fixed conformation are referred to as Intrinsically Disordered Proteins (IDP).

As millions and millions of copies of each protein are made in a lifetime, random events may lead these molecules to follow a wrong pathway and misfold eluding cellular quality control mechanisms (2). Under appropriate conditions, proteins with known native structures and without (IDP´s) can misfold prompting them to self-aggregate into amyloid fibrils (3). Such "renegade" protein aggregates can be closely related to cytotoxicity.

1.2 Protein Misfolding in Amyloidosis - "The Highway to Hell"

Amyloidosis refers to a variety of conditions where proteins misfold aggregating into amyloid fibrils. The deposition of these insoluble aggregates in organs and tissues *in vivo* is a hallmark of amyloid-related disorders (4). In recent years, many of these neurodegenerative disorders have gained an increase in interest due to a rapidly rising costly issue in terms of health care and social disruption (4). This diverse group of disorders has effects that are felt in every part of the body and every part of the globe (1).

Classification of amyloid diseases is dependent on the protein identity and their deposition pattern as insoluble amyloid aggregates (Table 1). The accumulation of amyloid fibrils is linked to a diverse set of diseases including Parkinson´s disease

(PD), Alzheimer´s disease (AD), Diabetes Type II, Huntington´s disease and many others (3, 5).

Table 1. Classification of some amyloid disorders in respect to protein identity and deposition pattern as amyloid fibrils.

Clinical Disease	Amyloid-Forming Peptide	Location of Amyloid Formation
Parkinson's disease	α-Synuclein	Brain
Alzheimer´s disease	Amyloid-β (Aβ) Tau	Brain
Huntington´s disease	Huntingtin	Brain
Transthyretin Amyloidosis	Transthyretin	Systemic
Diabetes Type II	Islet Amyloid Polypeptide	Pancreas

1.3 Parkinson´s Disease – "The Shaking Palsy"

James Parkinson was the first to clinically describe PD as the Shaking Palsy in his published monograph in 1817 (6). Since then many advances have been made in the direction of understanding the pathology. Today, it is suggested that the symptoms of PD are a result of loss of dopamine neurons in the *Substantia Nigra,* located in the midbrain region, accompanied by intraneuronal inclusions (7). In an early course of disease, the most common symptoms are movement-related, such as shaking, rigidity and slowness of movement. Later on, cognitive and behavioral problems, as well as, dementia may arise.

PD neurodegeneration results from the accumulation of intercellular and intracellular deposits of amyloid aggregates, which are termed Lewy bodies and

Lewy Neurites. The main component of these inclusion bodies is a protein known as α-synuclein (α-syn). In addition, other proteins and lipids have also been identified as components of Lewy bodies (8, 9).

PD is a multifactorial disease; both genetic and non-genetic factors are involved (9). In approximately 95% of PD cases there is no apparent genetic linkage ("sporadic" PD), with the remaining 5% of the cases being inherited (10). There are many mechanisms suggested to be involved in the development of PD, such as, accumulation of misfolded protein aggregates, incompetent protein clearance, mitochondrial dysfunction, oxidative stress, excitotoxicity, neuroinflammation and genetic mutations (9). Both the formation of Lewy bodies and the spreading of the pathology throughout the brain are hallmarks of PD (11).

1.4 α-Synuclein - "Peptide from Hell"

The phrase "peptide from hell" has been commonly used by scientists who on a daily basis endure the demeanor of Aβ (12). Having had the privilege to work with both Aβ and α-syn peptides, I can say without a doubt that the description "peptide from hell" also fits α-syn to perfection. α-Syn can be found both as an intrinsically disordered peptide in the cytosol but also with an α-helical conformation when associated to lipid membranes (13). It is therefore suggested based on its dynamic structure, to play specific roles in different cellular locations (13). The function of α-syn is not entirely understood but the protein has been suggested to be associated with the synapse and involved in synaptic activity, synaptic plasticity, neurotransmitter release, dopamine metabolism, synaptic pool maintenance and vesicle trafficking (14). Interestingly, the overexpression of α-syn both in humans (15) and in animal models (16) leads to much greater toxic effects than those caused by loss of α-syn (14, 17).

α-Syn is a 140 amino-acid long acidic protein with three domains: an N-terminal lipid-binding region, a hydrophobic central domain and a C-terminal acidic tail (Figure 1). Positively charged residues are located mainly in the N-terminal region (residues 1-60). The lipid-binding region of α-syn also contains 7 amino-acid sequence repeats containing the highly conserved KTKEGV motif, which is also present in the α-helical domain of apolipoproteins (13). These repeats are responsible for the ability to form α-helical structures and therefore important in α-syn-lipid interactions. When associated to anionic vesicles α-syn forms a linear helix with the first 100 amino-acid residues involved in the α-helical structure (18-20). All identified mutations associated with synucleinopathies are located in this lipid-binding domain: A30P, E46K, H50Q, G51D, A53E and A53T (14).

The central hydrophobic region (residues 61-95), also known as Non-amyloid-β component (NAC), is particularly rich in hydrophobic residues and makes up the core region of amyloid fibrils as it forms cross-β structures (13). Peptides derived from the NAC amino-acid sequence are capable of forming ordered fibrils and can seed Aβ1-40 and Aβ1-42 aggregation (21, 22). Interestingly, the strong fibril formation propensity of α-syn is not shared by its homologue β-syn, which lacks 11 hydrophobic residues in the NAC region (23). β-Syn was shown unable to form amyloid fibrils (23).

The C-terminal domain (residues 96-140) is highly concentrated with acidic amino-acids. The sequence of the C-terminal tail is homologous with small heat shock proteins. It has been suggested that the highly charged C-terminal tail may have a protective role in fibril formation (13). Lowering the negative charges at the C-terminal region, by lowering pH (11) or by truncations of the C-terminal has been shown to accelerate aggregation (24, 25).

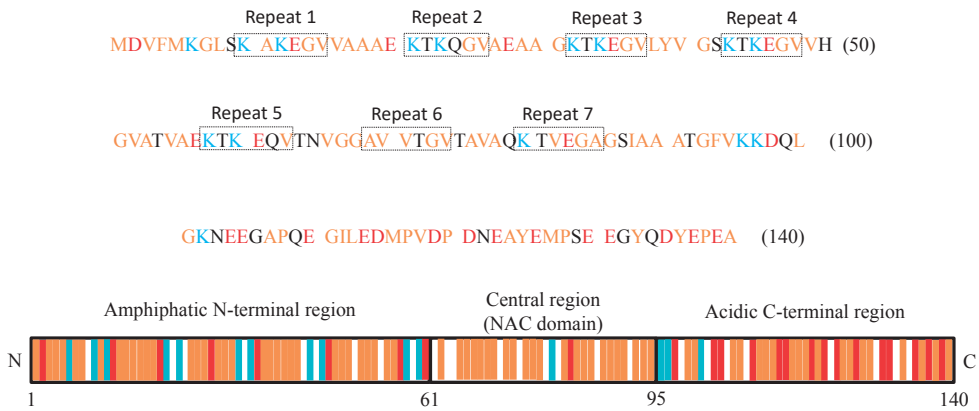

Figure 1. α-Syn sequence and charge residue distribution profile. The acidic residues are highlighted in red, the basic in blue and the hydrophobic in orange. The 7 amino-acid sequence repeats containing the highly conserved KTKEGV motif are boxed.

In aqueous solution, recombinant monomeric α-syn is unfolded (Figure 2).

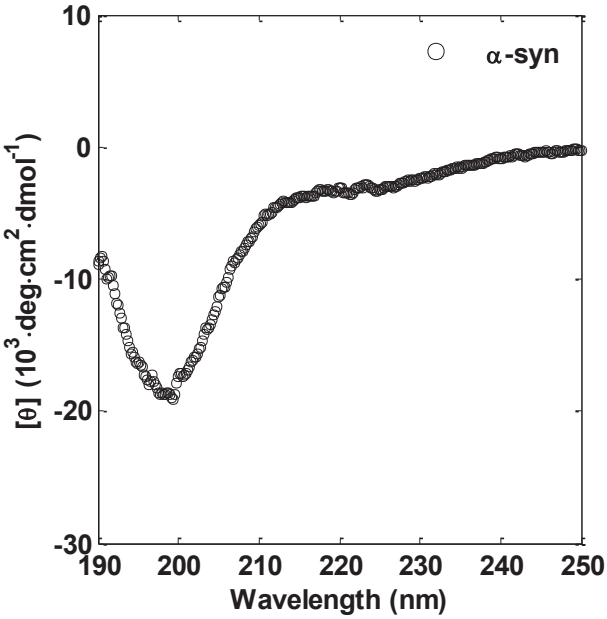

Figure 2. Secondary structure of monomeric α-syn monitored with Far UV circular dichroism spectroscopy in 10 mM MES buffer pH 5.5. The spectrum displays a minimum around 200 nm, which is typical for a protein in random coil, i.e. with no defined structural element (Paper V; 54).

1.5 Amyloid Fibril – "*Amylum*"

Amyloid fibrils are supramolecular structures discovered 150 years ago, that were shown to be stronger than steel, flexible as silk, highly resistant to degradation and with the capability to preform essential functions in many living systems (4). The term amyloid was introduced in 1854 by Rudolph Virchow. Examining brain tissue with abnormal appearance, he mistakenly concluded after positive iodine staining that the macroscopic defects consisted of starch. He named these starch-like structures amyloid, from the Latin word for starch - *Amylum*. The modern definition for amyloid fibril protein is that it occurs in tissue deposits as rigid, unbranched fibrils with the ability to bind Congo red dye and exhibit birefringence when viewed by polarization microscopy (26). When analyzed by X-ray diffraction, the fibrils should exhibit the characteristic cross-β diffraction pattern (26), with repeating substructure units consisting of β-strands running perpendicular to the fiber axis (27). Notable observations from the diffraction pattern are a spacing of 4.7-4.8 Å between hydrogen bonded β-strands within a

sheet and 6-11 Å between the β-sheets (28, 29). Amyloid fibrils tend to be long (> 1 μm) and rather thin (10-20 nm in diameter) structures.

Recombinant α-syn has been shown to form amyloid fibrils. I have had during my PhD the opportunity to image α-syn fibrils using different experimental techniques, such as, cryo-EM and super resolution microscopy (Figure 3).

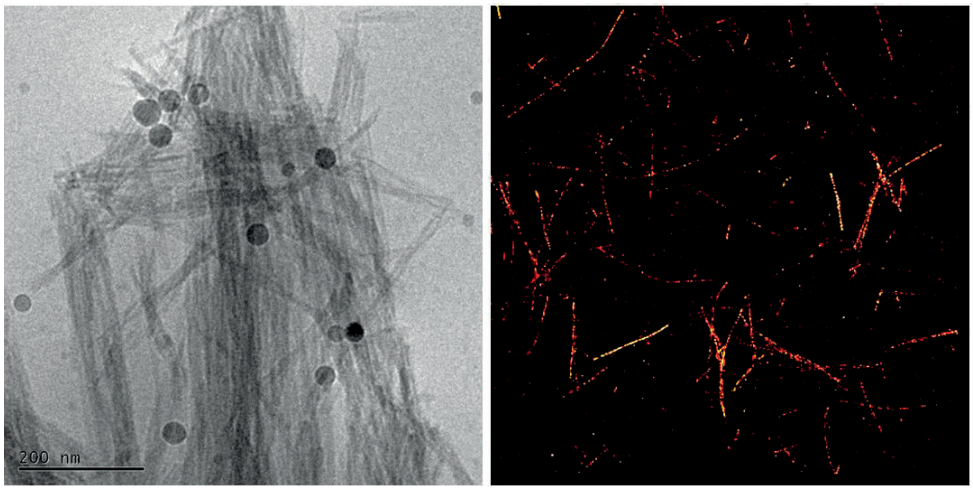

Figure 3. α-Syn amyloid fibrils. α-Syn amyloid fibrils imaged using cryo-EM **(left panel)** and dSTORM super resolution microscopy **(right panel)**. Important to point out, the circular shaped objects in the left panel are artefacts. Images published in Paper II.

Increasing evidence suggests that the amyloid state may be more stable than the functional native state of many protein molecules (30). The propensity for amyloid formation depends on amino-acid sequence and solution conditions (1). Mature protofibrils are the first structures to exhibit amyloid characteristics. These protofibrils twist around one another giving origin to higher order amyloid fibrils (31).

As many proteins and peptides have the ability to fold into amyloid fibrils it may indicate that fibril formation is not necessarily sequence specific, and can be driven purely on backbone interactions, limited by the steric hindrance associated with the packing of side-chains on both sides of the β-sheet (32). The assembly of protofilaments into fibrils seems to be driven by hydrophobic side-chains that are exposed on the sides of the amyloid core (5). These non-specific hydrophobic interactions can lead to polymorphisms within the amyloid fibers. Polymorphic fibrils can differentiate on the degree of twisting, the number of filaments per fibril

and the diameter of the fibril (33). It has been suggested that different polymorphic structures have different biological functions and contribute to different cytotoxicity levels (33).

1.6 Amyloid Cytotoxicity

Protective mechanisms are used and are associated with properties of the cellular environment to conserve proteostasis. Such "housekeeping" mechanisms include molecular chaperones, unfolded protein response pathways, protein degradation by proteasomes and autophagy that serve to avoid accumulation of misfolded and aggregated protein at all various stages in the lifecycle of proteins (4, 30, 34). The role of fibrils in amyloid diseases is still unclear. Amyloid fibrils have been suggested to be toxic themselves, or contribute to cytotoxicity by acting as reservoirs of toxic oligomers, or generating the formation of oligomeric species on their surface through secondary nucleation or by disrupting protein homeostasis (35-40). Many emerging studies claim oligomers to be the toxic mediators for cell damage and cytotoxicity (4). Oligomeric species have gained much interest, but have proven to be challenging to study due to their often transient and dynamic nature. Adding to this and further complicating structural analysis of oligomers, is the intrinsic heterogeneity found in these species, both in variability of size and structure (41).

Various amyloid-forming proteins seem to share similar cytotoxic mechanisms, independent of whether their aggregates are formed inside or outside of the cell (42, 43). For this reason, it has been commonly suggested that these protein aggregates may share a common target, the cell membrane (42, 43).

1.7 Aggregation Mechanism – "From Macroscopic to Microscopic"

Kinetic approaches towards determining mechanisms of protein aggregation began with work of Oosawa *et al* on actin polymerization using the monomer-addition model (44). Ferrone *et al* in the 1980s introduced the concept of filament fragmentation and heterogeneous nucleation, which was suggested to take place on the surface of existing aggregates (45). A simplistic view of the protein aggregation process and it´s complex network of microscopic events can be divided into three types of reactions (46):

- only dependent on monomers
- only dependent on aggregates
- dependent on both monomers and aggregates

Primary pathways only involve monomers. If nucleation occurs between monomers in the bulk solution it is referred to as homogeneous primary nucleation, opposing to nucleation that occurs at an external surface which is then referred to as heterogeneous nucleation (47). Primary pathways lead to the formation of larger aggregated species (Figure 4). As soon as these initial aggregated species are present, secondary pathways need to be accounted for. Examples of secondary pathways are fragmentation and secondary nucleation. Fragmentation, an event only dependent on aggregated species, generates new aggregates producing new fibril free ends, which can further elongate by the addition of new monomers (Figure 4). This event is prominent, in particular, when mechanically shaking the reaction sample as this leads to breakage of fibrils. Secondary nucleation requires both monomer and aggregated species. Secondary nucleation consists of an initial attachment of monomers to the surface of an amyloid fibril, followed by nucleus formation and detachment (Paper II). Secondary nucleation increases rapidly both the load of oligomeric species and fibrils. As a result of a high rate constant for secondary nucleation, nuclei generated from secondary nucleation usually dominate over primary nucleation from very early in the aggregation reaction an onwards (48).

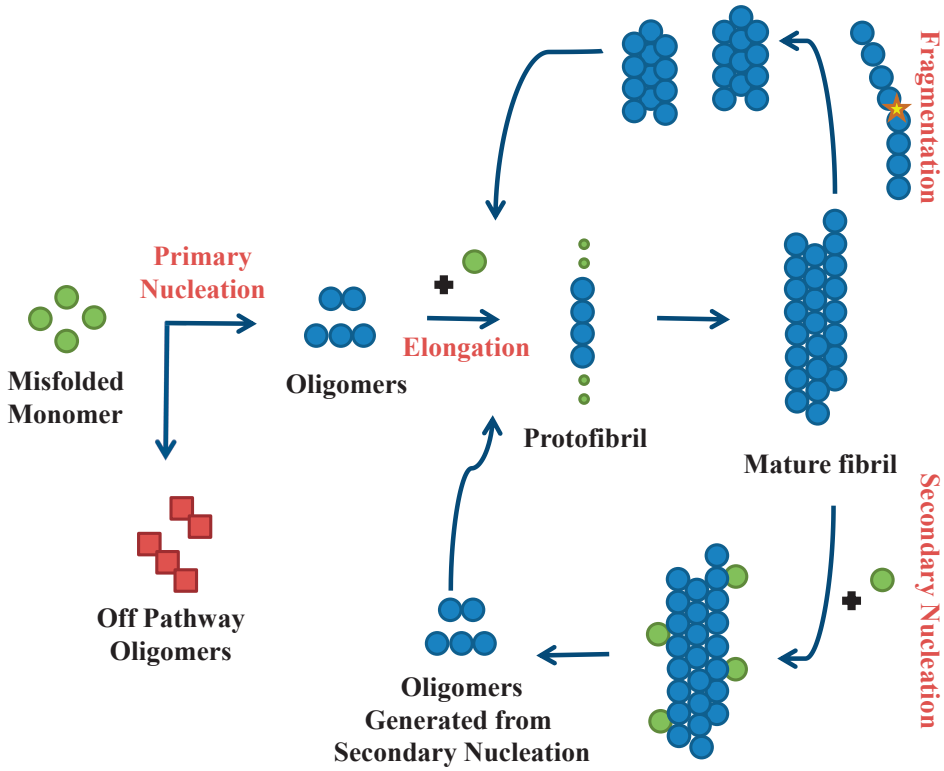

Figure 4. Simplistic illustration of the microscopic events present in protein aggregation. The events are often divided into three types of reactions: only dependent on monomers (Primary nucleation); only dependent on aggregates (Fragmentation); dependent on both monomers and aggregates (Secondary nucleation and Elongation).

1.8 Monitoring aggregation kinetics with thioflavin-T

Thioflavin-T (ThT) was introduced by Vassar and Culling in 1959. ThT is a cationic benzothiazole dye that shows enhanced fluorescence upon binding to cross-β structures (49, 50). It is very commonly used to diagnose both *ex vivo* and *in vitro* amyloid fibrils, as well as, following fibril formation (50). The critical micellar concentration of ThT in water was obtained to be around 4 μM (49). ThT molecules have been shown to bind to amyloid fibrils and this is accompanied by enhanced fluorescence with excitation and emission maxima at approximately 440 and 490 nm, respectively (49-51). The detailed binding mechanism of ThT to amyloid fibrils is still not fully understood. The most accepted view is that ThT molecules are intercalated within the side-chain channels of the amyloid fibrils that run along the fibril axis (50, 52). This rigid environment results in a rotational immobilization of the central C-C bond connecting benzothiazole and aniline

rings, giving rise to enhanced fluorescence (50, 52). The minimal binding site has been suggested to require four consecutive β-strands (52).

As mentioned above the formation of fibrils occurs through a nucleation-dependent polymerization reaction. Underlying the macroscopically observable typical ThT sigmoidal trace (Figure 5) are various possible microscopic events occurring simultaneously at different rates: primary nucleation of monomers in the bulk solution or at a surface, elongation of fibrils through monomer addition, monomer-dependent secondary nucleation and fragmentation. A common parameter to describe ThT kinetic aggregation traces is $t_{1/2}$, which is the time at which the ThT fluorescence reaches 50% of the total fluorescence intensity.

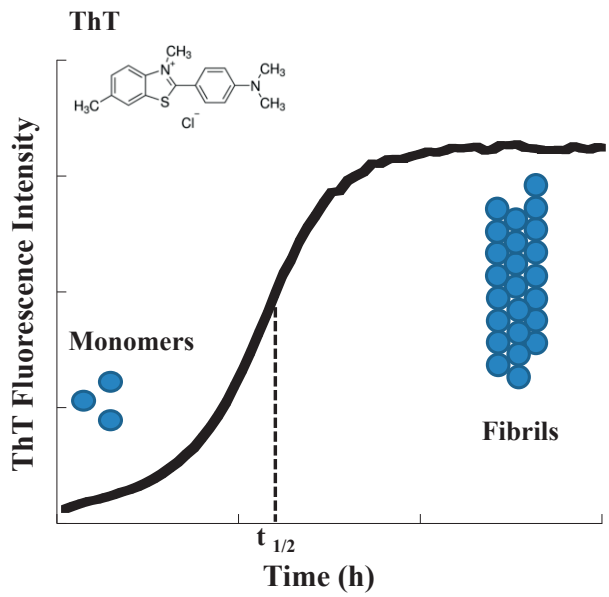

Figure 5. A typical sigmoidal amyloid aggregation trace for α-syn monitored by ThT.

The ability to fit macroscopically observed kinetic traces and extract detailed information of microscopic events and rate constants can be extremely valuable (53). This approach has shown capable of capturing the mechanistic details for many amyloid-forming proteins, as long as, it includes the accurate microscopic steps and rate constants (Paper I and II, 24, 25, 37, 46, 54). The quantitative information in terms of rate constants of each microscopic step and how they vary depending on protein sequence, solution conditions and additives can therefore be attained.

1.9 Lipid Membranes

1.9.1 Model Membranes

Model membranes are simplified systems composed of a small set of defined components found in membrane systems *in vivo* allowing us to control physical-chemical parameters of interest, such as, membrane charge, lipid specificity, lipid headgroup size and acyl-chain packing. A lipid bilayer can adopt different phases depending on temperature, pressure, hydration and structural properties of the lipid composition (55, 137). The liquid disordered bilayer is characterized by a low acyl-chain order and high lateral diffusion (56, 57). The liquid crystalline lamellar phase differs from so-called gel phase bilayers were the chains have crystalline packing. The transition between gel and liquid crystalline lamellar phases depend on properties of the lipid molecules including length and unsaturation of the chain, as well as, size and charge of the lipid headgroup. The liquid ordered bilayer structures occur in many lipid mixtures containing cholesterol. The liquid ordered lamellar phase is characterized by a high order in the acyl-chain region without losing the high lateral diffusion (56, 57). In order to investigate the interaction of α-syn to lipid membranes, experiments were conducted using model membranes. Our studies focused mainly on physiologically relevant lipids but also some model lipids that are not commonly found in biological systems but were chosen because of their molecular characteristics (Figure 6).

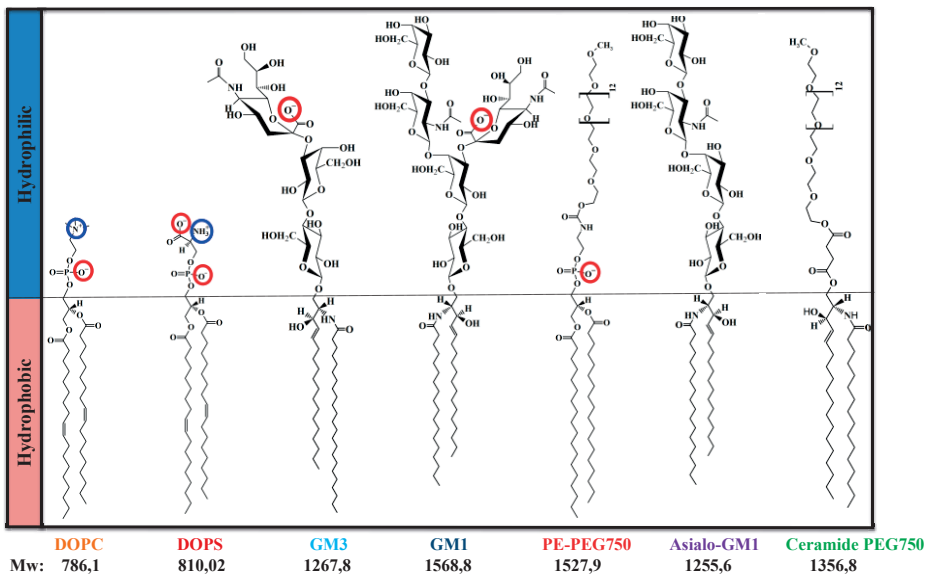

Figure 6. Chemical structures of the main lipid species investigated.

These amphipathic lipids self-assemble into a variety of arrangements, exhibiting a variety of different structures. The structure of such assemblies is dictated by the chemical nature of the lipids and the surrounding conditions. For the various experiments performed during my PhD, different lipid self-assembled structures where studied, including systems that form lamellar bilayer phases and micelles. In the studies with bilayer-forming systems, dispersed unilamellar vesicles, deposited bilayers or bilayer lipodiscs were used (Figure 7).

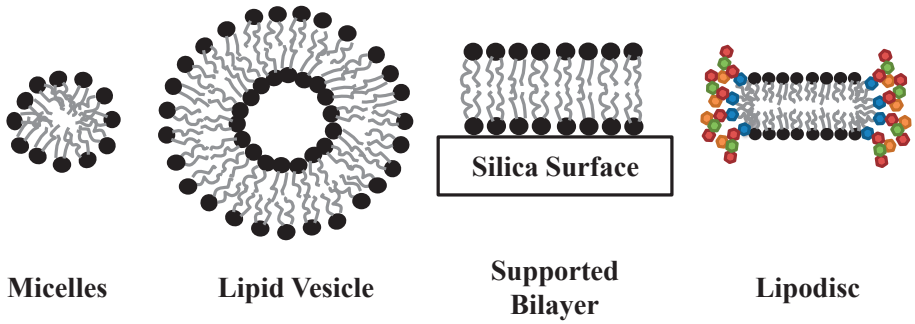

Figure 7. Lipid self-assembled structures used for model membrane studies.

1.9.2 The Cell Membrane

The cell membrane is a semi-permeable barrier that serves to protect the integrity of the interior of the cell or organelles, allowing certain molecules in and keeping others out. In a typical eukaryotic cell it has a thickness of ca. 5 nm. The cell membrane is primarily composed of lipids and proteins. The lipid composition is complex and varies between organelles and the plasma membrane. Lipid composition also varies between the inner and the outer leaflet in, for example, the plasma membrane (58). Some examples of lipids commonly found in the outer leaflet of the plasma membrane are Sphingomyelin, Cholesterol and Glycolipids (such as, Gangliosides (GM)) (59). In the inner leaflet, Phosphatidylethanolamine (PE), Phosphatidylserine (PS) and Phosphoinositides (PI) are more frequent (59). Cardiolipin (CL) is found in the inner leaflet of mitochondria (58). Phosphatidylcholine (PC) is common in all cellular membranes.

The fluid mosaic model proposed that biological lipids form a uniform and homogeneous mixture in the plane of the bilayer (60). Much has evolved since this model was originally formulated. The lipid raft hypothesis suggests that lipids are sorted into domains, lipid rafts, which are rich in sphingolipids (for example gangliosides) and cholesterol (61). The phase coexistence of liquid-ordered and

liquid-disordered phase in lipid rafts confers these domains unique physicochemical properties (60, 61). There are studies suggesting that lipid rafts act as preferential interaction sites for amyloid peptides leading to pathological forms of the peptides (60).

1.10 Protein-Lipid Interaction and Co-Aggregation

The function of α-syn is not yet fully understood. There seems to be a striking similarity with amyloid-forming apolipoproteins at the level of primary and secondary structure, in the sense that both protein families have repeating sequences that give rise to lipid-binding α-helical domains (62). Due to the location of α-syn in neurons, it is widely assumed that α-syn may modulate the dopamine neurotransmission by regulating synaptic vesicle trafficking (63). Interesting, albeit the adipose tissue, neural tissue has the second highest content in lipids. The interaction of α-syn and lipid membranes are highly relevant, and there are different aspects of protein-lipid interactions that are important, some of which have been investigated in this PhD thesis:

- For several of the amyloid disorders, protein aggregation has been associated with membrane disruption in cells and in model membranes (18, 64-68). Therefore, the effects of α-syn on lipid membranes, such as, membrane permeabilization and membrane thinning are of interest.

- Lipid membranes are reported by numerous studies to influence the protein aggregation process (54, 69, 70). The effect of lipid membranes on α-syn aggregation mechanism was here investigated in papers IV, V and VII.

- Tightly associated lipids have been identified in amyloid plaques associated with several amyloidogenic diseases from *in vivo* and *in vitro* studies (42, 71-81). Interactions between lipids and amyloid peptides may modulate the aggregation, but also the structure and physical-chemical properties of the co-aggregates formed. Co-aggregation implies extraction of components from the lipid membrane which in turn is likely to affect membrane structure and function (74). Structure of α-syn-lipid co-aggregates was studied in paper VI.

- It has been suggested that α-syn is able to form lipid-protein particles reminiscent of high density lipoproteins, linked to the transport of α-syn across the blood-brain barrier (82-85). Formation/stabilization and characterization of such α-syn-lipid assemblies is highly relevant.

2.Methodologies

The goal of this PhD thesis is a detailed characterization of the amyloid aggregation mechanism of α-syn. Focus will be on the protein α-syn alone, as well as, in the presence of model membranes of different lipid compositions, and biological membranes in exosomes isolated from Neuroblastoma cells. In this section a brief overview follows of some methodologies and experimental techniques used.

2.1 α-Synuclein Protein Preparation

For all experiments described, we used human α-syn expressed in *E. coli* from a Pet3a plasmid containing a synthetic gene with *E. coli*-optimized codons (purchased from Genscript, Piscataway, New Jersey), and purified using heat treatment, ion exchange and gel-filtration chromatography. A key procedure to achieving reproducible experiments is to use pure samples as starting material. Gel-filtration is a crucial step to isolate pure monomeric α-syn in the desired degassed experimental buffer. Only protein sample corresponding to the central region of the peak is collected. Freshly purified peptide samples were prepared and handled always on ice to avoid initiation of the aggregation process. The peptide concentration was determined by absorbance at 280 nm using an extinction coefficient $\varepsilon = 5800\ l \cdot mol^{-1} cm^{-1}$.

2.2 Small Unilamellar Lipid Vesicle Preparation

The procedure for preparation of small unilamellar vesicles (SUV) was the same for all experiments. Stock solutions of lipids were prepared by weighting and mixing lyophilized lipids accordingly, in chloroform/methanol 2:1 v/v. Thin lipid films were deposited onto glass vials under a slow flow of nitrogen and further dried in a vacuum oven at room temperature overnight. The lipid films were then rehydrated with experimental buffer to a final pre-determined concentration. Sonication of the SUVs was done using a microtip, 50 % duty cycle for 15 min at 65 % amplitude, followed by centrifugation for 3 min at 13000 g. The size of the SUVs was checked often by dynamic light scattering and was shown to be ~80 nm in diameter.

2.3 Monitoring α-Synuclein Aggregation Kinetics using ThT

In order to monitor α-syn fibril formation using ThT some important experimental aspects were initially addressed (Paper II and unpublished data):

- Can ThT be used to quantify relative amyloid fibril amounts?
- What is the optimal concentration of ThT to monitor α-syn aggregation?
- Does ThT affect the aggregation process?

Conversion of the fluorescence signal to aggregate mass requires that the signal intensity is proportional to the amount of fibrils formed. ThT affinity and quantum yields are influenced by several factors therefore preliminary optimization studies were necessary for our solution conditions (36). A set of samples containing different amounts of α-syn seeds were titrated with a concentration variation of ThT (Figure 8). The first observation was that fluorescence intensity from ThT dye bound to the fibril is proportional to the amount of fibrillar mass in a defined regime of dye concentrations (Figure 8). The fluorescence of the dye decreases at higher dye concentrations which is likely due to self-quenching.

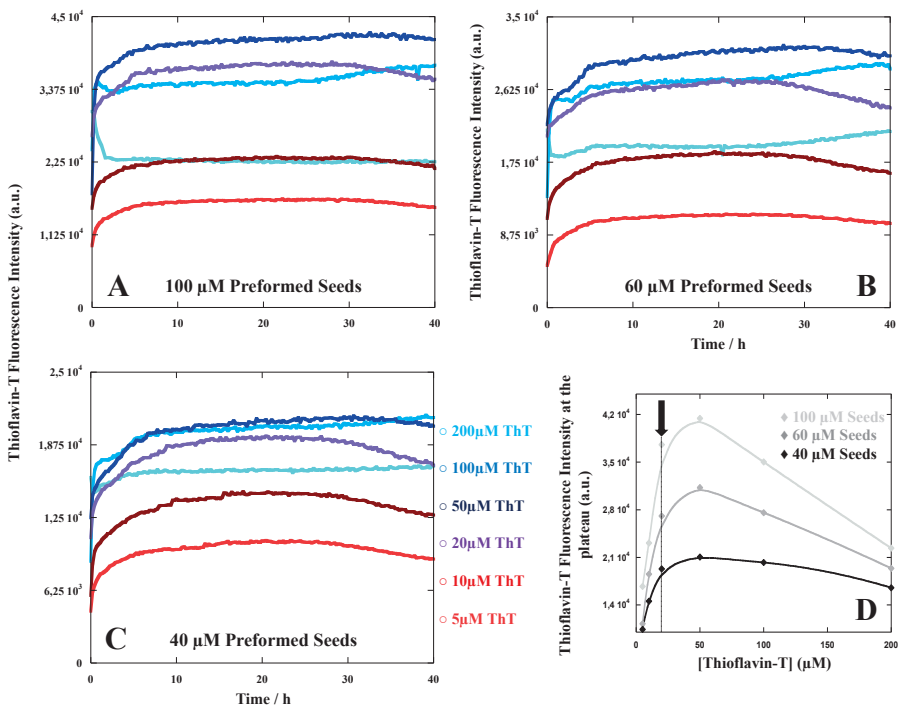

Figure 8. ThT titration of different concentrations of α-syn seeds. A) 100 µM **B)** 60 µM and **C)** 40 µM seeds were titrated with ThT in 10 mM MES buffer pH 5.5 at 37°C under quiescent conditions. The figures show average ThT

kinetic traces that are shown in bold and are plotted as ThT intensity as a function of time. **D)** ThT fluorescence intensity at the plateau plotted as a function of the respective ThT concentration for each seed concentration tested. Arrow and dotted line indicate the optimal concentration for ThT (20 µM) accessed to have a linear relationship between fluorescence intensity and aggregate concentration (Paper II).

In order to monitor α-syn fibril formation, the concentration of ThT has to be optimized for the protein concentration range investigating. It is crucial that the concentration of ThT in the sample is sufficient, so that fluorescence intensities are meaningful and not influenced by complete depletion of ThT from the solution at high concentrations of α-syn fibrils (Paper II).

A typical ThT seeded kinetic α-syn aggregation experiment is shown in Figure 9. The fluorescence intensity of 20 µM ThT increases as a function of time, indicative of an increase in the amount of β-sheet enriched structures. To support this, parallel to an increase in ThT signal is a decrease in monomeric α-syn present in the sample as a function of time, measured by absorbance at 280 nm. These results nicely show that an increase in aggregate concentration is paralleled by a decrease in monomer concentration.

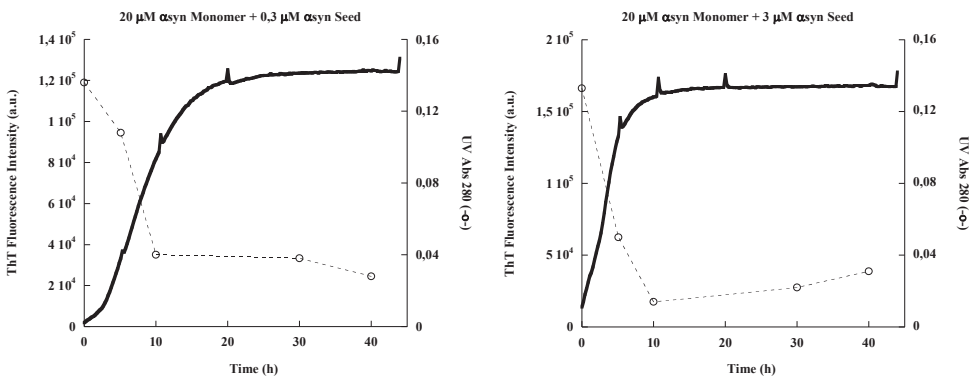

Figure 9. Aggregation kinetics of α-syn. The aggregation kinetics of 20 µM α-syn in the presence of two seed concentrations, **(right panel)** 3 µM and **(left panel)** 0.3 µM, followed using ThT (bold lines) and in parallel monitored by measuring the concentration of α-syn remaining in solution as a function of time using absorbance at 280 nm (dotted lines; unpublished data).

2.4 Trap and Seed Kinetic Assay

The trap and seed kinetic assay is based on a typical seeding experiment (Figure 10). The method was designed to identify the dominant secondary process of α-syn aggregation. To perform such an assay, there are some experimental details to improve reproducibility which will be briefly described below. The first detail is to evaluate the influence of the surface material of the filter plates on α-syn

aggregation, and this was performed simply by incubating α-syn monomer in such plates, filtrating and monitoring the aggregation kinetics with ThT in a plate reader at 37 ºC. No aggregation was seen during the time frame investigated when using low-binding GHP membrane filter plates.

Prior to the experiment, the filter plates are washed with experimental buffer to remove any contaminants. The membrane filter is also rinsed with α-syn monomer until one saturates the membrane. The experiment is performed following 3 steps:

Step 1:
Once the pre-treatment of the filter plates is done, the first step of the experiment is to trap fibrils in the filter plate. α-Syn fibrils were trapped by filtration applying vacuum. The flow-through (Filtrate 1) is collected in a non-binding PEGylated plate supplemented with ThT and aggregation kinetics monitored in a plate reader. If the trapping has been successful the ThT fluorescence intensity in filtrate 1 should be similar to the background.

Step 2:
The trapped fibrils are then incubated for a certain period of time with monomer, buffer or other component. In the experiments published in Paper II, freshly purified α-syn monomer and experimental buffer were added and incubated with the trapped fibrils for 2 h. As a reference sample, the monomers where incubated in buffer solution without any seeds for the same period of time.

Step 3:
After the incubation period, the samples are newly filtered and the flow through collected in PEGylated plates, supplemented with ThT and monitored in the plate reader (Filtrate 2).

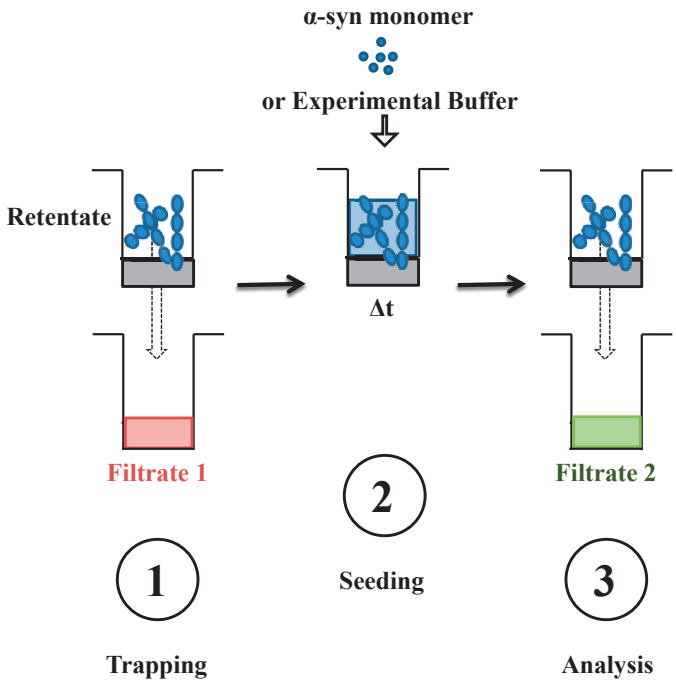

Figure 10. Schematic representation of the experimental steps involved in the trap and seed aggregation kinetic assay.

2.5 Phosphorus Assay

Phospholipid concentrations were determined by phosphorus analysis according to Rouser *et al*. For this assay, α-syn was aggregating in the presence of phospholipid vesicles of different compositions. A solution of KH_2PO_4 was used in order to obtain a standard phosphorus concentration curve. Extremely important to highlight is that all glassware used for this assay was properly washed with detergent containing no phosphorus. Before usage of the glassware, it was rinsed with 1% Nitric acid. The concentration of α-syn was kept constant at 0.5 mg/ml with the concentrations of lipid vesicles varying from 0 to 1 mg/ml. These samples were left aggregating overnight at 37 ºC in an orbital shaker at 200 rpm. Each sample was then centrifuged for 5 min at 13000 g. Representative volumes of the supernatant were collected in glass vials. The pellet was resuspended in buffer and representative volumes were also collected for analysis. All collected samples were placed in a heat block at 115 ºC to evaporate the solvent. Dried samples were then digested with 0.65 ml Perchloric acid 70 % at 180 ºC for 20 min and left cooling. When cool, 3.3 ml milliQ H_2O, 0.5 ml 25 g/l ammonium molybdate and

0.5 ml 100 g/l ascorbic acid were added to the samples. The samples were placed for 5 min at 100 ºC and immediately after the absorbance was read at 800 nm.

3.Experimental Techniques

3.1 Size-Exclusion Chromatography

Size-exclusion chromatography (SEC) is a method that allows separation of molecules based on their size. The chromatography column is packed with porous beads, such as, dextran polymers or agarose. The sample is applied to the column and the pore structures of the resin will provide a molecular sieve. In this method the efficiency to penetrate the pores of the stationary phase is measured, meaning that small molecules will access the entire volume of the beads while bigger molecules are excluded from the pores. Having said this, larger molecules are eluted first with the smallest last (Figure 11).

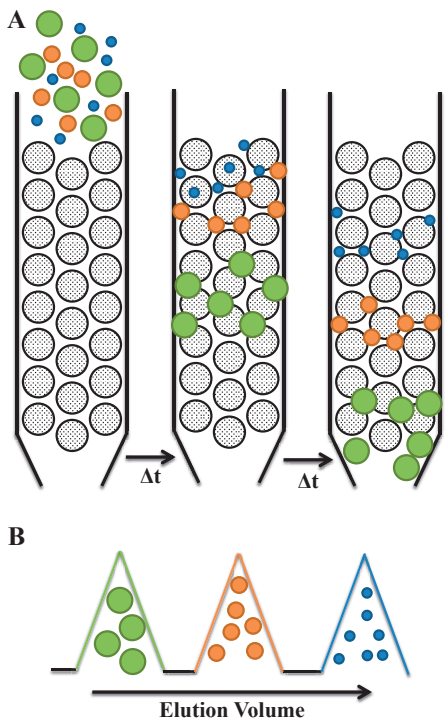

Figure 11. Schematic illustration of size-exclusion chromatography. The porous beads are colored in light grey. **Panel A** shows the evolution of the separation of three molecules of different sizes: green circles the largest molecules, orange intermediate size and blue the smallest. In **panel B**, it is shown the order of which the molecules will elute as a function of elution volume.

3.2 Fluorescence Spectroscopy

Fluorescence is a luminescence phenomenon where certain molecules emit light upon absorption of photons from a light source. Fluorescence is thus a photon emission phenomenon. Most molecules occupy the lowest vibrational level of the electronic ground state. Absorption of incoming photons will promote the molecule to an electronic excited state. This excitation to an emissive state will only occur when the wavelength of an incident photon matches the energy difference between the vibrational ground state of the electronic ground state and a vibrationally excited state of the electronically excited state. This is because the absorbance of the photon and excitation of the electron happens much faster than the time scale of inter-nuclear vibrations, and excitation goes to one or more vibrationally excited levels that have the largest overlap with the ground state wave function. In the excited state, collisions with other molecules cause the excited molecule to lose vibrational energy and drop down to the lowest vibrational level of the electronically excited state. The molecule then travels back to a vibrationally excited state of the electronic ground state emitting a photon. Due to the relaxation, the photon emitted is of lower energy than that of the initially absorbed photon, which is referred to as the Stokes shift. Here, fluorescence spectroscopy was used to detect and quantify the presence of fibrils through the interaction of ThT (all Papers). Also used to visualize the aggregation process using protein molecules with different fluorescent labels (Paper II).

3.3 Circular Dichroism Spectroscopy

Circular Dichroism (CD) spectroscopy measures the differential absorption of left *vs* right circularly polarized light (86, 87). The vast majority of biological molecules are chiral. 19 of the 20 common amino acids that build up proteins are also chiral. As a result of proteins containing chiral chromophores, left and right circularly polarized light will be absorbed differently. CD of molecules is measured over a range of wavelengths. Far UV CD spectra of proteins reveal characteristics of their secondary structure while near UV monitor changes in tertiary structure. Typical CD spectra of α-helix, β-sheet and random coil are shown in Figure 12. Here, circular dichroism spectroscopy was mainly used to monitor changes in α-syn secondary structure in the presence of lipid membranes with different compositions (Papers V).

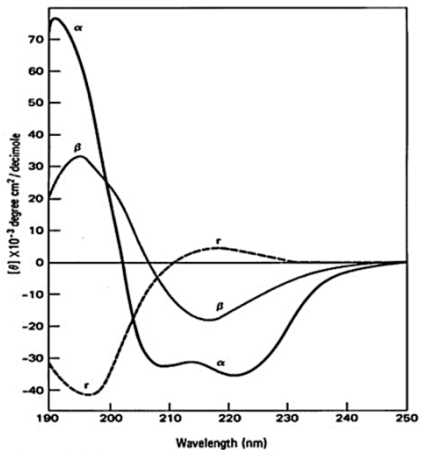

Figure 12. Characteristic α-helix (α), β-sheet (β) and random coil (r) signature CD spectrum. Figure adapted from T. E. Creighton, *Proteins*, W. H. Freeman 1984.

3.4 Cryo-EM

Cryo-EM is extremely useful since the amyloid fibrils to be visualized do not need to be in a crystalline form neither labeled with stable isotopes or dyes (28). Electrons produced by an electron gun are transmitted through the sample. As electrons have shorter wavelengths compared to photons, higher resolution can be achieved when compared to a light microscope. The sample is spread on a carbon coated copper grid forming a thin layer and plunged into liquid ethane at -180ºC in a temperature and humidity controlled environment. It is very important that the freezing of the sample is rapid as it prevents the frozen water around the molecules from forming cubic ice, and enables the trapping of the molecules structure in the transparent amorphous ice. Here, cryo-EM was used to investigate the structural evolution of α-syn aggregates formed in the presence of lipid membranes (Papers IV and VI)

3.5 Super Resolution Fluorescence Microscopy (dSTORM)

Spatial resolution has been limited by the diffraction of light restricting our view to length scales of 200-300 nm in the lateral direction and 500-700 nm in the axial direction. Super resolution fluorescence microscopy has allowed to overcome the diffraction barrier enabling an optical resolution of ~20 nm.

Direct stochastic optical reconstruction microscopy (dSTORM) is one of these super resolution microscopy techniques. It relies on the different temporal emission of fluorescence from fluorophores. Fluorophores close-by emit light at different times allowing them to be resolved if separated by a distance that exceeds the light diffraction limit. The photoswitching of single fluorophores and tunable transition rates are key for dSTORM. An excitation beam excites randomly fluorophores that may convert after several blinking cycles to a dark state. A second beam then excites stochastically fluorophores into a bright state. The basis of dSTORM falls on the ability to spatially and/or temporally modulate the transition between a fluorescent bright state and a photoreduced dark state. dSTORM was here used to investigate α-syn amyloid growth from seed fibrils at mildly acidic pH conditions (Paper II).

3.6 Quartz Crystal Microbalance – Dissipation

Quartz crystal microbalance with dissipation (QCM-D) is a surface sensitive tool, which provides real-time information on adsorption processes where the measured signals depend on both adsorbed amount and how much these molecules extend out in the surrounding solutions. The method is often commonly used to study lipid bilayer deposition and protein binding to lipid membranes (88). A QCM-D sensor is a thin piezoelectric quartz crystal in-between a pair of electrodes, usually made of gold. The electrodes can be coated with different materials, such as, silica oxide. The sensor is excited to oscillate at its resonance frequency by applying an alternating voltage. During an experiment, several resonance frequencies, referred to as overtones, are monitored.

The mass of the adsorbed layer is sensed as a change in the resonance frequency of the oscillating crystal (Δf) (88, 89). When molecules adsorb to an oscillating quartz crystal, water or other liquids also couple to the adsorbed mass. The frequency will decrease with an increase of the adsorbed "wet mass". The viscoelastic properties of the film are deduced from the damping of the sensor movement, meaning changes in dissipation. Dissipation occurs when the voltage to the crystal is shut off, and the energy of the oscillating crystal dissipates (ΔD) (88, 89). Measuring the dissipation parameter is analytically useful for films of adsorbed molecules that extent into the solution and which do not follow the linear relationship between measured frequency shift and adsorbed mass. The dissipation increases for films with high coupling to the solution. Here, QCM-D was used to investigate α-syn adsorption to lipid membranes varying both lipid compositions and solution conditions (Paper VII), as well as, adsorption of α-syn to preformed fibrils (Paper II).

3.7 Differential Sedimentation

Sedimentation of particles in a liquid is vastly used to characterize particle size distribution. Particles with different densities sediment at different rates in the liquid in which they are suspended in. The sedimentation rates will depend on several factors, such as, liquid viscosity, particle shape and size and the force used to sediment (gravitational or centrifugal).

By measuring the time it is necessary for particles to settle a known distance in a liquid of known viscosity and density, it is possible to determine the corresponding particle size distribution. It is common to apply Stoke´s law for spherical particles. Using the disc centrifuge apparatus in paper II, sedimentation occurs via centrifugal force, extending the possible range of particle separation down to about 5 nm. Ultimately, the disc centrifuge method relies on the fact that α-syn aggregates of different sizes travel through a sucrose gradient at different speeds. However, there are some deviations to Stoke´s laws, and to us the most problematic was the fact that α-syn aggregates are not spherical particles. It is reported that the errors associated to the diameters measured for particles with large aspect ratios or very irregular shapes, such as α-syn aggregates, may not exceed 20%. Although the size obtained is to some extent unreliable, the size distribution profile still contains important qualitative information. Here, differential sedimentation was used to identify the nature of the dominant secondary process of the aggregation mechanism of α-syn at slightly acidic pH solution conditions (Paper II).

4.Results and Discussion

The aim of my PhD thesis was to characterize the aggregation mechanism of α-syn in the absence and presence of lipid membranes. The following chapter discusses some of the major questions investigated:

- Is α-syn aggregation kinetics reproducible? To investigate the aggregation mechanism of α-syn a reproducible method is required void of extrinsic interference (all Papers and unpublished data).

- How do solution conditions determine the relative importance of nucleation and growth processes in α-syn aggregation? α-Syn *in vivo* is in contact with different cellular environments with different pH lumens. It is therefore relevant to investigate the importance of pH on the aggregation mechanism of α-syn (Paper I).

- What is the underlying dominant secondary process of α-syn aggregation mechanism at mildly acidic pH conditions? At mildly acidic pH conditions secondary processes were shown to be enhanced. The nature of the dominant secondary process underlying the aggregation mechanism was identified (Paper II).

- What governs surface-assisted nucleation? Amyloid fibrils are often linked to cytotoxicity as a result of oligomeric species generated through surface-assisted secondary nucleation. Here, we investigated the importance of electrostatic interactions in secondary nucleation (Paper VII).

- What is the role of crystallin chaperones on α-syn fibril formation? Amyloid disorders are often linked to the disruption of the chaperone mechanism as a result of aging. Having said this, the role of crystallin chaperones and there effect on the aggregation mechanism of α-syn was evaluated in detail (Paper III).

- How to investigate the effect of lipid membranes on the aggregation kinetics of α-syn? We study protein-lipid interactions as we believe that this may affect the fibril formation process due to protein-membrane association. For this one needs a reproducible method to monitor protein-lipid co-aggregation (Paper IV-VII and unpublished data).

- How do biological membranes influence α-syn aggregation? Cell-to-cell transfer of α-syn involving exocytosis/endocytosis mechanisms has increasingly gained

interest. We investigated the effect of biological membranes in exosomes on the aggregation mechanism of α-syn (Paper IV).

- What lipid headgroup features drive α-syn association to lipid membranes? Lipid membranes where shown to influence α-syn association and aggregation. We investigated whether the effects observed are related to specific headgroup interactions or if it is attributed to more generic properties of the lipid headgroup, such as, charge and size (Paper V and unpublished data).

- Do lipids affect the morphology of the protein-lipid co-aggregates? The formation of protein-lipid co-aggregates will have distinct structure, morphology and dynamics compared to assemblies of either protein or lipid alone. Protein-lipid co-aggregates during the course of the aggregation process were monitored using cryo-TEM (Paper VI).

- Are lipids taken up into amyloid aggregates during the co-aggregation process? Here we investigated if lipids are taken up to the final protein-lipid co-aggregate using a range of different lipid model systems (unpublished data).

4.1 Is α-synuclein aggregation kinetics reproducible?

The reproducibility of ThT kinetic experiments is crucial for investigating the mechanism of α-syn aggregation. α-Syn aggregation has been shown to be strongly influenced by intrinsic and extrinsic factors. In order to better understand the role of some extrinsic factors, the effect of surface materials of the sample containers on α-syn aggregation was investigated. Other factors that were previously shown to play a role are air-liquid interfaces (90), temperature (91), pH (Paper I), salt concentration (Paper VII, 92) and the presence of cofactors (93). Knowing what external factors strongly interfere with α-syn aggregation enables us to further design experimental conditions where we avoid such interference.

To investigate the role of surface materials, reactions starting from monomeric peptide under quiescent conditions were monitored by ThT at mildly acidic pH in two of the most common sample containers used in kinetic studies of amyloid formation: Untreated polystyrene plates and non-binding plates coated with PEG (PEGylated plates). In polystyrene plates the aggregation kinetics of α-syn revealed to be reproducible, and this is the reason why initial studies (for example presented in Paper IV) were all performed in such sample containers (Figure 13B; Paper II). On the other hand, in PEGylated plates, the aggregation of α-syn was shown to be extremely slow and not observable up to 100 h (Figure 13A; Paper II).

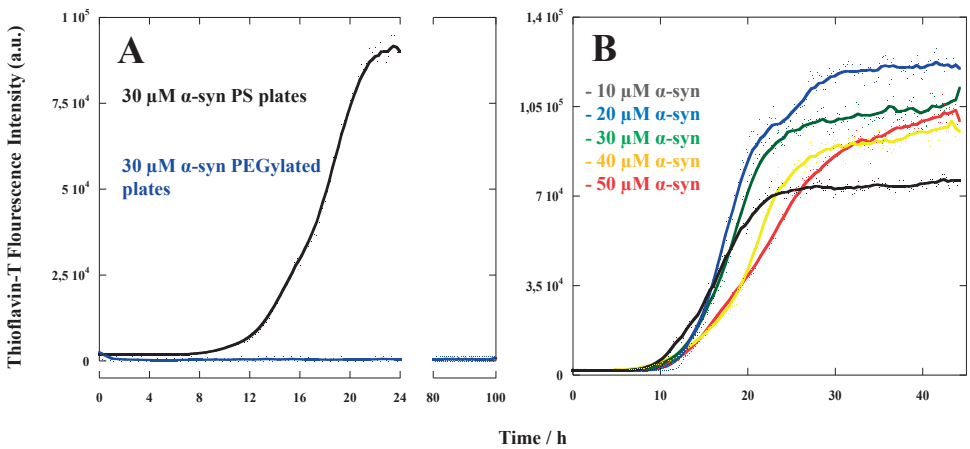

Figure 13. Role of surface materials on α-syn aggregation. A) Aggregation kinetics of 30 µM α-syn in polystyrene plates and in non-binding PEGylated plates. **B)** α-Syn aggregation kinetics for different monomer concentrations, ranging from 10 to 50 µM in polystyrene plates. The aggregation kinetics monitored in polystyrene plates appears quite independent of the peptide concentration, suggesting that the available polystyrene surface may be a limiting

factor. Experiments were performed in 10 mM MES buffer pH 5.5 under quiescent conditions at 37ºC. The average traces are shown in bold in the figures with experimental repeats dotted (Paper II).

Nucleation and Fragmentation can be selectively enhanced

To further understand the catalytic nature of polystyrene surfaces, plain polystyrene nanoparticles (24 nm diameter) were added to monomeric α-syn in PEGylated plates under quiescent conditions (Figure 14, unpublished data). With the addition of polystyrene nanoparticles, aggregation occurs to similar extent as that in polystyrene plates (Figure 14). This implies that it is indeed through an interaction of monomeric α-syn and polystyrene that aggregation is induced by triggering heterogeneous primary nucleation (Figure 15; 94, Paper II). Interestingly, higher concentrations of nanoparticles caused slower aggregation kinetics, possibly due to a greater surface adsorption resulting in a decrease of α-syn concentration (Figure 14). When the concentration of nanoparticles is increased, the concentration of α-syn also needs to increase for aggregation to be observed.

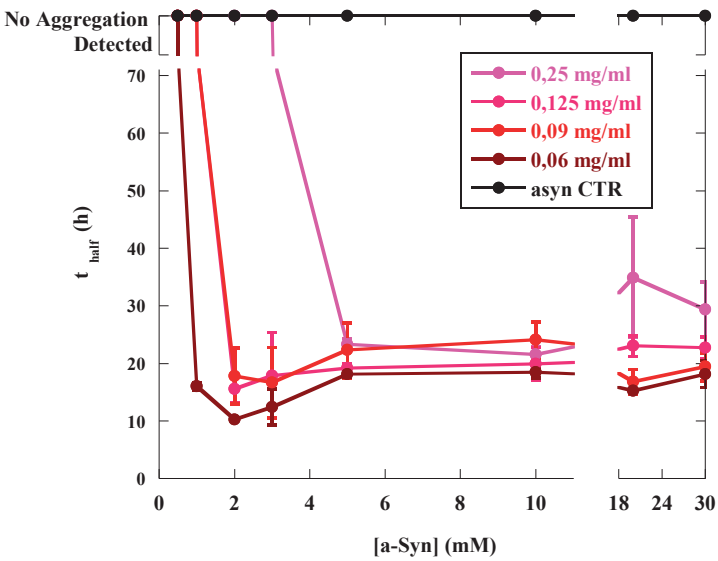

Figure 14. Polystyrene surfaces selectively enhance heterogeneous primary nucleation. α-Syn aggregation kinetics for different monomer concentrations, ranging from 1 to 30 μM in the presence of different concentrations of polystyrene nanoparticles. Experiments were performed in PEGylated plates in 10 mM MES buffer pH 5.5 under quiescent conditions at 37ºC. The figure shows the average $t_{1/2}$ for at least 3 experimental repeats for each condition. At low monomer concentrations it appears that all peptide may be adsorbed to the nanoparticles, for example, monomer concentrations 1, 2 and 3 μM in the presence of 0.25 mg/ml polystyrene nanoparticles, no aggregation is observed (unpublished data).

It should be mentioned that many studies in literature have resorted and still resort to other approaches to trigger α-syn aggregation, such as, mechanical shaking of the samples or other extrinsic factors mentioned above. However, these external parameters will affect the aggregation mechanism of α-syn. In particular, the effect of shaking has been investigated, highlighting some associated complications as will be discussed later in this thesis. In short, shaking has been shown to selectively enhance both nucleation and fragmentation leading to rapid aggregation kinetics (Figure 15). Shaking induces the formation of air-liquid interfaces (e.g. bubble formation), which induces α-syn to adopt α-helical conformation at the interface, favoring fibril formation (90, 95).

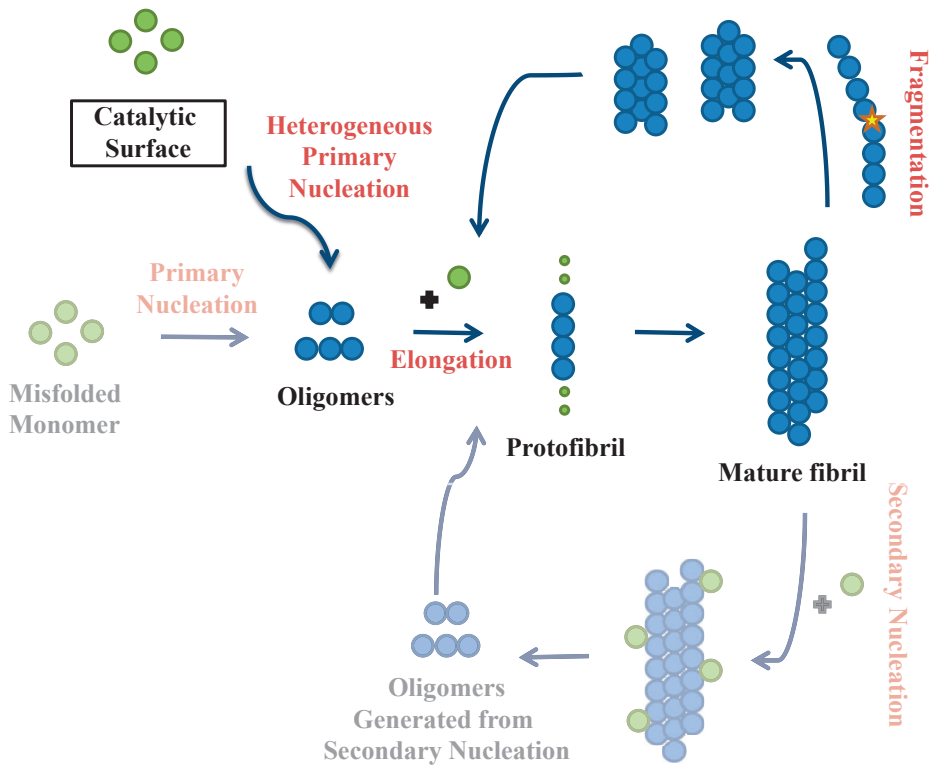

Figure 15. Extrinsic factors, such as hydrophobic surfaces and shaking, selectively enhance heterogeneous primary nucleation and fragmentation. The microscopic events that are enhanced due to extrinsic factors are highlighted in the figure. One should however point out that the microscopic events shaded in the figure still occur during the aggregation process.

Seeded kinetics, the way we prefer for experiment reproducibility

Although the high reproducibility and rapid aggregation kinetics observed in polystyrene plates, it is hard to interpret, as the observed effects are affected by the interaction of α-syn with the polystyrene surface. Having said this, to characterize the aggregation mechanism, kinetic experiments were performed in the absence of foreign catalytic surfaces in PEGylated plates, were α-syn aggregation is extremely slow due to an undetectably low primary nucleation rate constant. Triggering aggregation in such sample containers was possible with the addition of, for example, preformed α-syn fibrils, and often referred to as seeds. Seeds were added to the reaction solution in known amounts (counted as monomer equivalents). The addition of seeds bypasses the need for primary nucleation (Figure 16). The lagtime is a direct consequence of the amount of seeds added to the aggregation reaction. The lagtime decreases with increasing amounts of seeds. The reaction is very sensitive to the concentration and size of the seeds, it is vital to handle all seed solutions in the same manner (Paper II).

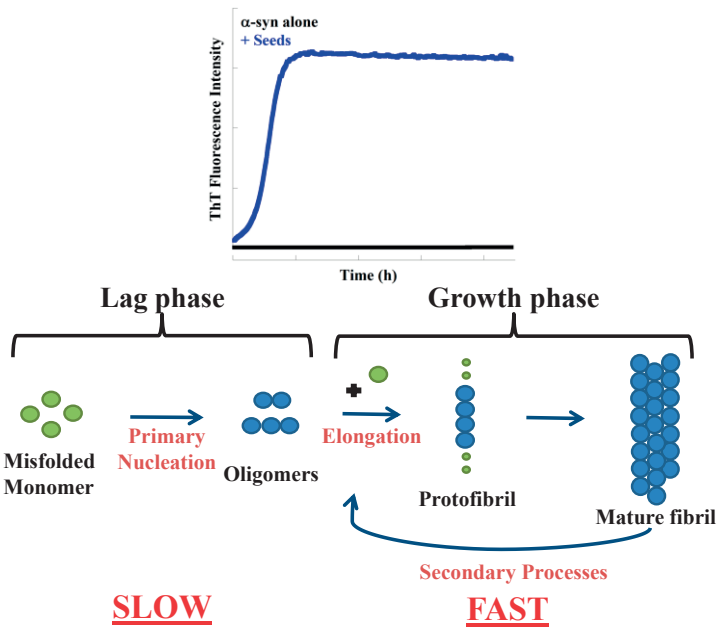

Figure 16. Seeded Aggregation kinetics in non-binding PEGylated plates. The addition of seeds triggers α-syn aggregation by enhancing secondary processes leading to reproducible aggregation kinetics and bypassing the need for primary nucleation.

Conclusion:
In the lab we are able to reproduce the aggregation kinetic data for α-syn and other amyloid-forming peptides quite effortlessly when our starting samples are pure (all Papers). This clearly highlights the non-stochastic feature of the aggregation process in bulk samples.

4.2 How do solution conditions determine the relative importance of nucleation and growth processes in α-synuclein aggregation?

An extremely interesting feature of α-syn is the fact that this peptide displays a highly polarized charge distribution. As a result of this heterogeneous distribution of charges within the amino acid sequence of α-syn, its aggregation behavior is strongly dependent on solution conditions, such as, pH and ionic strength. As α-syn is in contact with different cellular environments with different pH lumens, it is physiologically relevant to evaluate the importance of pH on the aggregation kinetics.

I should point out that at the time of this study we were conducting aggregation kinetic experiments at mildly acidic pH. We learned that the research group in Cambridge was doing similar experiments at neutral pH (96). We then decided to merge efforts and follow the aggregation as a function of pH. The approach was to systematically vary monomer concentrations in the presence of different seed concentrations and vary pH of the solution (from pH 5.5 to 6.5) (Figure 17, Paper I and VII).

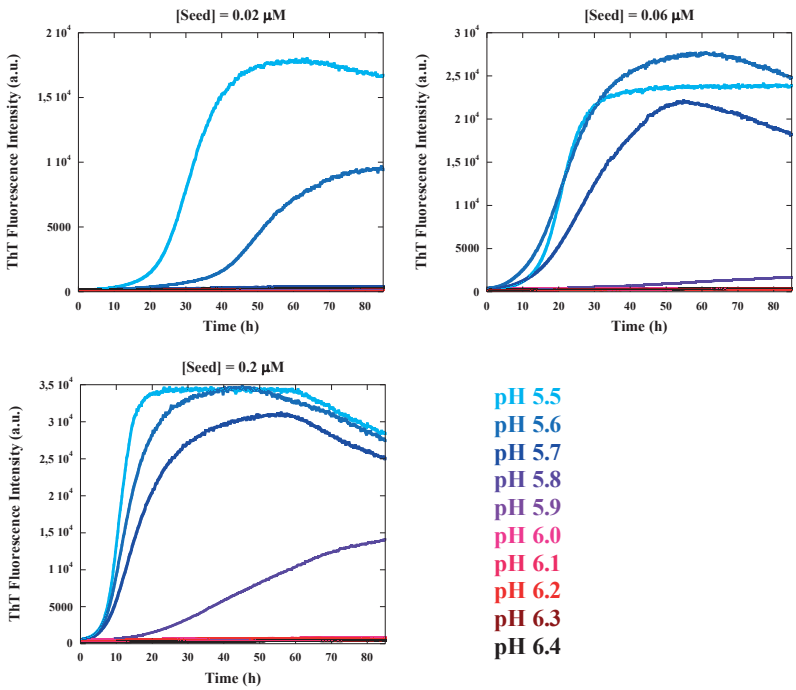

Figure 17. **pH dependence of the aggregation kinetics of α-syn at low ionic strength**. Aggregation kinetics of 20 µM α-syn monomer was monitored varying the pH from 5.5 to 6.4 in 10 mM MES buffer for three different seed

concentrations ranging 0.02, 0.06 and 0.2 μM under quiescent conditions at 37ºC. The figure shows average traces of at least three experimental repeats (Paper I and VII).

Conclusion:

The experiments were performed by different people in different labs in different countries but revealed to be highly reproducible and congruent. The aggregation mechanism was shown to change as a function of pH. At neutral pH, the rate constant of elongation and higher-order assembly of fibrils was much higher than that of primary nucleation and secondary processes (Figure 18). Below pH 6 secondary processes are enhanced and strongly accelerate the aggregation kinetics of α-syn changing the overall character of the aggregation process (Figure 18). Secondary processes manifest themselves through a positive curvature of the measured sigmoidal ThT kinetic aggregation trace (Figure 17). These findings in Paper I provide new insights into possible mechanisms of α-syn aggregation at different pH-values, which might have impact on understanding the spreading in the context of PD. Establishing correlations between solution conditions relevant to specific cellular compartments and overall aggregation profiles and propensity of α-syn can help understand the prion-like mechanism.

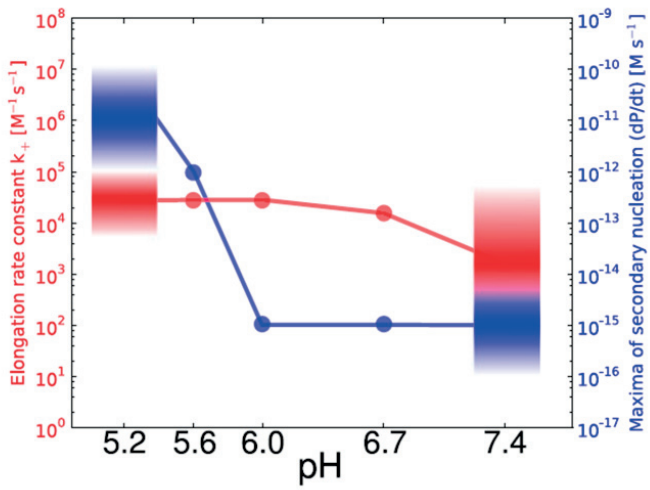

Figure 18. **Elongation rate constant and maximal fibril production through secondary nucleation as a function of pH** (Paper I).

4.3 What is the underlying dominant secondary process of α-synuclein aggregation mechanism at mildly acidic pH conditions?

We have seen that the overall balance of nucleation and growth is altered as a function of pH. At acidic pH conditions secondary processes were shown to be enhanced. The effect is manifested by a very strong acceleration of the aggregation in the presence of seeds. Through a multitude of experiments, the aggregation mechanism was studied in order to distinguish between two possible secondary processes: fragmentation of fibrils or nucleation of monomers on the surface of existing aggregates.

Distinguishing between Fragmentation and Secondary nucleation

The two kinetic models for dominant fragmentation or dominant monomer-dependent secondary nucleation processes are expected to give rise to very similar ThT kinetic traces as confirmed by simulations (Paper II). Therefore, to distinguish between both secondary processes a set of different experimental approaches were used:

- Differential sedimentation analysis was performed to study how the size of fibrils changes over time after the aggregation reaction has finished. No spontaneous fragmentation of fibrils was observed over a 20 day period.

- Incubating monomeric α-syn for short time periods with trapped fibrils, followed by filtration lead to acceleration of the aggregation (trap and seed experiment, see section 2.4). This finding implies the formation of oligomeric species consistent with secondary nucleation of monomers on the fibril surface. These generated oligomeric species are small enough to pass through the filter membrane and seed the aggregation reaction.

- dSTORM enabled us to visually confirm secondary nucleation (Figure 19). Incubating, α-syn preformed seeds labeled with Alexa Fluor 647 (red color) with α-syn monomer labeled with Alexa Fluor 568 (green color), showed a coexistence of both colors along the fibril length and in some regions what appeared to be growth in green color from the seed in red color.

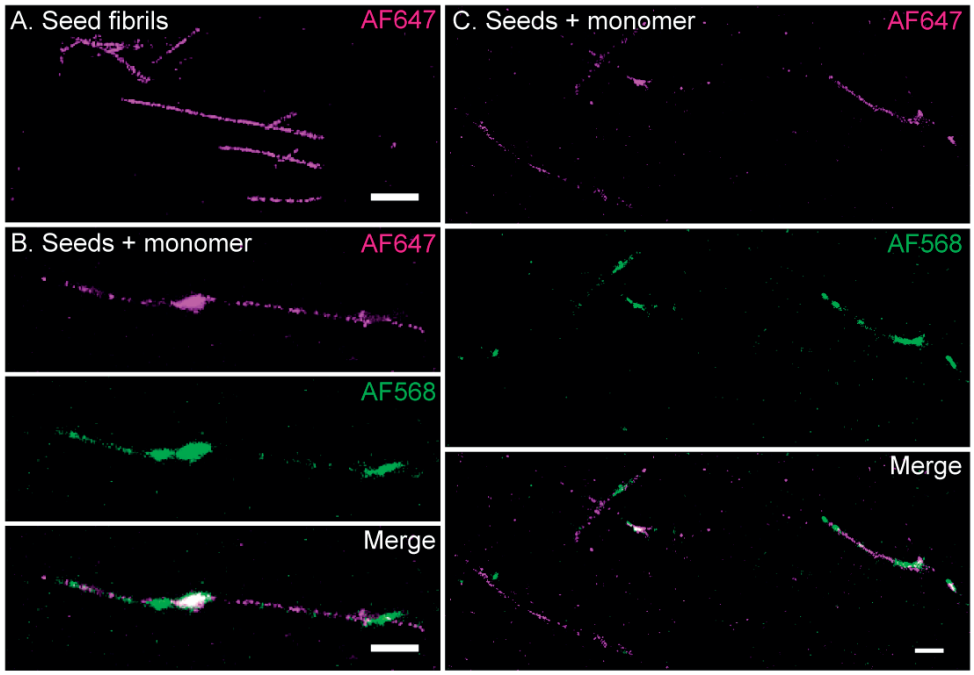

Figure 19. **dSTORM imaging of amyloid growth from seed fibrils at mildly acidic pH conditions. A)** Imaged seed fibril labeled with 1:20 Alexa Fluor 647 used for the self-seeding experiment. **(B, C)** α-syn monomer labeled with Alexa Fluor 568 was incubated with 50% seed fibrils labeled with Alexa Fluor 647. Top panel is imaged in the red channel, middle panel imaged in the green channel and lower panel is a merge between both channels. The scale bar corresponds to 1 μm (Paper II).

Conclusion:

Altogether, the results presented in paper II suggest that secondary nucleation of monomers on fibril surface dominates α-syn aggregation and provides an autocatalytic amyloid amplification mechanism. At mildly acidic pH, the overall net charge of α-syn is reduced compared to neutral pH, leading to an increase in the aggregation propensity. Both monomer concentration and the available fibril surface may be rate limiting for monomer-dependent secondary nucleation. Acidic pH is found in some intracellular compartments, namely linked to the endocytic and exocytic pathways, where multiplication of smaller species may therefore be much faster than at physiological pH.

4.4 What governs surface-assisted nucleation?

Much remains unknown in terms of surface-assisted nucleation and the molecular determinants for such microscopic events. We investigated the importance of electrostatic interactions for secondary nucleation by varying ionic strength. In addition, the effect of sequence mismatch was briefly studied through a cross-seeding kinetic experiment using two peptides of different sizes, α-syn and Aβ42.

The role of electrostatic interactions for secondary nucleation

To investigate the importance of electrostatic interactions for secondary nucleation, the aggregation kinetics at mildly acidic pH were monitored by ThT in the presence of a variation of ionic strength, ranging from 0 to 1200 mM NaCl for two different seeds concentration (Figure 20).

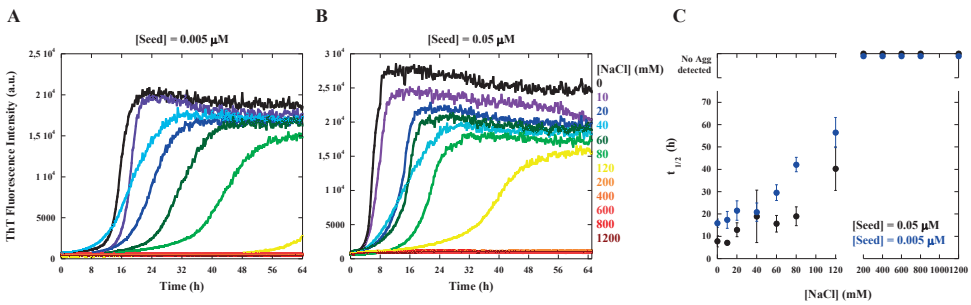

Figure 20. **Salt dependence on the aggregation kinetics of α-syn**. Aggregation kinetics of 5 μM α-syn monomer in the presence of two different seed concentrations, 0.005 **(A)** and 0.05 μM **(B)**, were monitored at salt concentrations ranging from 0 to 1200 mM NaCl added to the 10 mM MES buffer pH 5.5 at 37ºC under quiescent conditions. The figure shows the median traces of at least three experimental repeats. **C)** $t_{1/2}$ as a function of salt concentration for both seed concentrations (Paper VII).

Quite unexpectedly, paper VII shows that the addition of salt progressively retards the aggregation rate of α-syn with visible changes in the slope of the macroscopic ThT traces (Figure 20). This effect is contrary to that reported for other amyloid-forming peptides (97, 98). At high ionic strength, above approximately 120 mM NaCl, the aggregation seems to be completely inhibited for both seed concentrations during the time frame of the experiment.

The pKa values of the acidic residues, highly concentrated in the C-terminal tail of α-syn, are less up-shifted at increasing salt concentration, making this part of the protein more negatively charged at higher salt concentrations (Paper VII). This could in principle lead to greater repulsion between α-syn monomer and fibril

surfaces, however, this is compensated by the fact that there is more salt to screen the repulsion.

Another explanation to the anomalous salt dependence of aggregation involves the strongly anisotropic nature of α-syn charge distribution. If interactions between the positively charged N-terminal regions of α-syn monomers and the negatively charged C-terminal tails of α-syn decorating the fibrils, and *vice versa*, are critical for nucleation on the surface of the fibrils, then this attractive electrostatic component will be diminished upon screening by salt.

The role of sequence mismatch for surface-assisted nucleation

The effect of sequence mismatch was briefly studied through a cross-seeding experiment using α-syn and Aβ42. Both peptides have a slightly net negative charge at the chosen experimental solution condition, pH 5.5 (approximate isoelectric points for α-syn and Aβ42 are 4.8 and 5.3, respectively). One clear difference between these proteins is their size, where α-syn is a much larger peptide with 140 residues compared to Aβ42, with only 42 residues.

The experiment consisted of monitoring the α-syn aggregation kinetics with ThT of α-syn monomers incubated with preformed seeds of either α-syn or Aβ42. The data for Aβ42 are shown in figure 21. It can be observed that Aβ42 seeds, at two different concentrations 0.3 and 3 μM, were unable to seed aggregation of α-syn monomers (Figure 21). Seeds of α-syn, on the other hand, catalyzed α-syn aggregation at all concentrations investigated. This implies that surface-assisted nucleation is highly sequence specific and may only tolerate low level sequence mismatch.

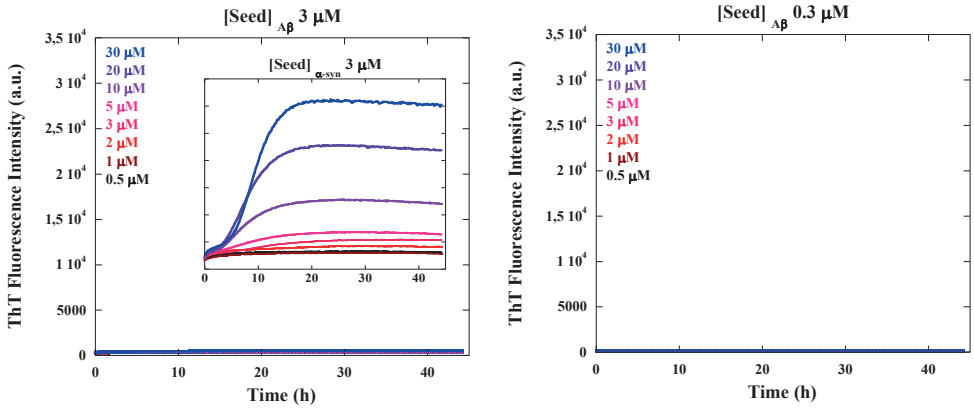

Figure 21. **Cross-seeding between α-syn and Aβ42.** Aggregation kinetics monitored by ThT starting from α-syn monomer at concentrations ranging 0.5 to 30 µM seeded with preformed fibrils of either α-syn or Aβ42 in 10 mM MES buffer pH 5.5 under quiescent conditions at 37ºC. The figure shows average traces of at least two experimental repeats (unpublished data; 136).

Conclusion:

It appears that homogeneous secondary nucleation is largely dependent on electrostatic interactions. Interactions between the positively charged N-terminal regions of α-syn monomers and the negatively charged C-terminal tails of α-syn seem critical for nucleation on the surface of fibrils.

Interestingly, there seems to be some sequence specificity critical for heterogeneous primary nucleation, tolerating only low levels of sequence mismatch, as Aβ42 fibrils were unable to trigger α-syn aggregation.

4.5 What is the role of crystallin chaperones on α-synuclein fibril formation?

Chaperones are of extreme importance for maintaining protein homeostasis. Chaperones have been vastly studied in the amyloid field and have been shown capable of inhibiting fibril formation for different amyloid peptides, such as, α-syn, PolyQ peptides, Aβ, among others by affecting different microscopic events (99-103). α-Crystallin displays chaperone activity and has been previously demonstrated to inhibit α-syn fibril formation at neutral pH conditions by affecting elongation (104). α-Crystallin is mainly found in the eye lens but also occurs in other tissues, such as, heart, skeletal tissue, kidney and brain (105). Studies have shown an upregulation in αB-crystallin in PD, Alzheimer´s disease and Creutzfeldt-Jacob disease (106).

As we have identified conditions governing reproducible aggregation kinetics, the effect of crystallin proteins on the aggregation of α-syn was investigated in paper III. Crystallin proteins were purified from bovine eye lens.

Crystallin protein family inhibits α-syn fibril formation

The aggregation kinetics of α-syn was monitored by ThT in the presence of seeds at three different concentrations and with a concentration variation of α-crystallin. α-Crystallin was shown to inhibit fibril formation. Curiously, when testing β- and γ-crystallin similar trends were observed with clear inhibitory effects.

Secondary Nucleation and elongation are inhibited in the presence of the Crystallin protein family

In order to understand the inhibitory effect of the crystallin protein family, a trap and seed experiment was performed. α-Syn seeds were pre-incubated with α- and γ-crystallin, trapped, and then incubated with freshly purified α-syn monomer. The α-syn seeds that were not incubated with crystallins had the effect to seed and accelerate the aggregation reaction (Figure 22). However, seeds that had been pre-incubated with either α- or γ-crystallin, were no longer capable of seeding the aggregation (Figure 22). The inhibitory effect seems to arise as a result of the interaction between crystallin and α-syn seeds, likely canceling secondary nucleation and elongation processes.

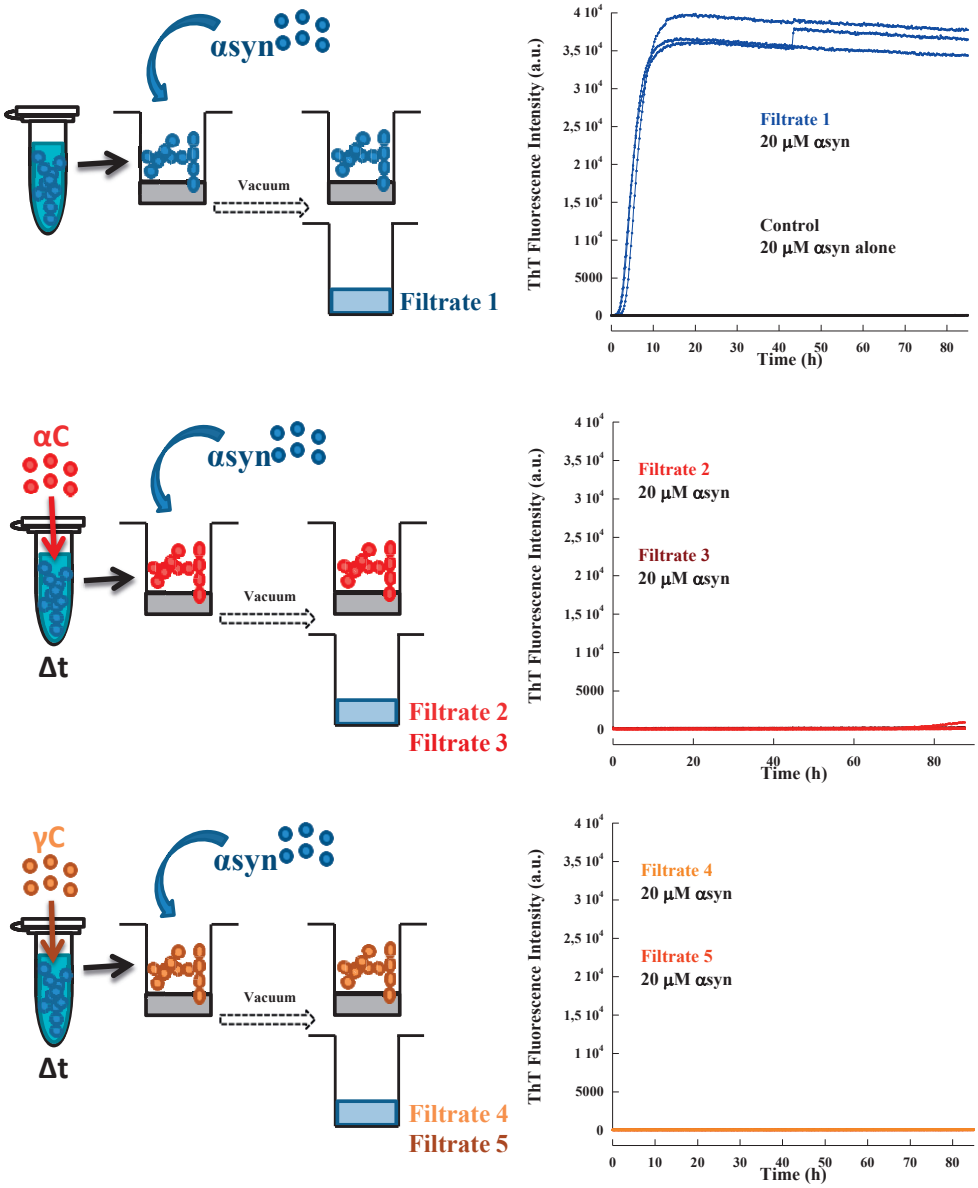

Figure 22. **Trap and Seed kinetic experiment.** 3 µM α-Syn seeds in 10 mM MES buffer pH 5.5 were trapped by filtration in filter plates. The trapped fibrils were then incubated for 2 h with freshly purified α-syn monomer and newly filtrated. The flow through was collected in PEGylated plates, supplemented with ThT and monitored in the plate reader (Filtrate 1). The same procedure was conducted with α-syn seeds pre-incubated for 2 h with two concentrations (0.2 and 2 mg/ml, respectively) of either α-crystallin (Filtrate 2 and 3) or γ-crystallin (Filtrate 4 and 5). The influence of the surface material of the filter plates was evaluated incubating α-syn monomer in the plates, filtrating and monitoring the aggregation kinetics with ThT in a plate reader at 37 °C under quiescent conditions. No aggregation was seen during the time frame investigated. The figures show the individual aggregation kinetic traces of three experimental repeats (Paper III).

The point of no return

The inhibitory effect of α-crystallin was also evaluated in an experiment where α-crystallin was added at different time points of the on-going seeded aggregation reaction. Interestingly, when α-crystallin was added before $t_{1/2}$ the aggregation of α-syn was either completely inhibited (highest concentrations) or inhibited to some extent (lowest concentrations). However, if α-crystallin was added after $t_{1/2}$, α-crystallin is no longer efficient in inhibiting/retarding α-syn aggregation. This result implies that the inhibitory effect is due to an interaction between crystallins and aggregated α-syn fibrils.

Conclusion:

The Crystallin protein family inhibits α-syn fibril formation at mildly acidic pH by inhibiting both secondary nucleation and elongation microscopic events. The inhibitory effect of α-crystallin was shown to be highly sensitive to the timing of when α-crystallin was added during the aggregation reaction.

4.6 How to investigate the effect of lipid membranes on the aggregation kinetics of α-synuclein?

As we have identified conditions governing reproducible aggregation kinetics, it is possible to investigate the role of lipid membranes on the aggregation kinetics of α-syn (107-109). In order to find good conditions to study the effect of lipid membranes and to make it possible to compare with different studies in literature, we first look into the role of surface materials of the sample containers and shaking *vs* quiescent conditions. Aggregation kinetics of monomeric α-syn in the presence of anionic DOPC/DOPS lipid vesicles was initially monitored with ThT in polystyrene plates and in glass vials at mildly acidic pH both under similar shaking conditions at 100 rpm (left vs middle panel, Figure 23). Not much difference can be seen for the aggregation profiles of α-syn alone and in the presence of DOPC/DOPS lipid membranes. One could be tempted to conclude that the sample container surface used to monitor aggregation is to some degree irrelevant. However, that is not the case. When repeating the experiment, in PEGylated plates and quiescent conditions (right panel, Figure 23), the effect of the same lipid systems above becomes more evident simply due to the fact that fragmentation is no longer dominating the aggregation process and there is limited interaction of α-syn with air-water interfaces at bubbles that appear due to shaking, and no interaction between α-syn and polystyrene catalytic surfaces. In such experimental conditions, no aggregation is detected for α-syn alone has previously described in section 4.1, while the anionic vesicles were shown to induce the aggregation reaction.

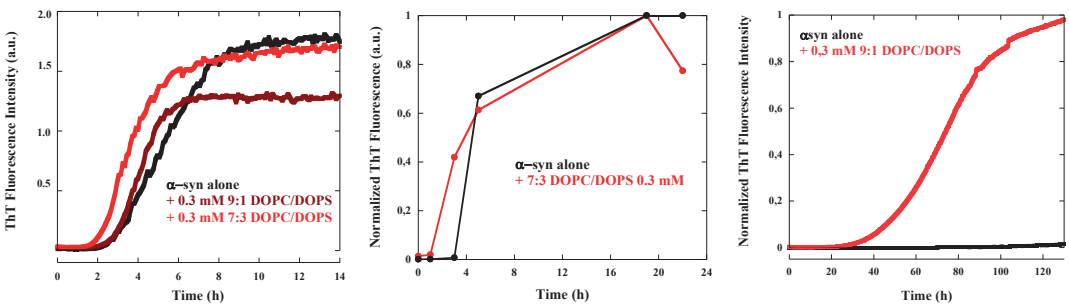

Figure 23. The role of extrinsic factors in α-syn aggregation in the presence of lipid vesicles. Aggregation kinetics of α-syn alone in the presence of anionic DOPC/DOPS vesicles was monitored by ThT at mildly acidic pH at 37ºC under shaking conditions in both **(left panel)** polystyrene plates and **(middle panel)** glass vials. (**right panel)** In addition, aggregation kinetics of α-syn alone and in the presence of anionic DOPC/DOPS vesicles was monitored under quiescent conditions in PEGylated plates at mildly acidic pH at 37ºC. The figures show average traces of at least three experimental repeats (unpublished data).

Figure 23 clearly illustrates the importance and effects of experimental conditions in terms of shaking and surface material when monitoring the aggregation kinetics of α-syn alone and in the presence of lipid membranes. Therefore, it is critical to perform all experiments in controlled conditions, which is done here for papers V, VI and VII. In paper IV, the different experimental conditions are compared, and conclusions are not drawn for retardation, while observed accelerating effects of lipids were attributed to the addition of the new component.

Conclusion:
This unpublished study concluded that PEGylated plates and quiescent conditions are the most appropriate experimental conditions to study the effect of lipid membranes on the aggregation of α-syn. This was the approach followed in the latter projects of this PhD thesis. With shaking, fragmentation becomes so dominant in the aggregation process that it often makes it hard to interpret results, independent of the sample container used.

Proof of Concept:

Monitoring the aggregation kinetics of α-syn titrated with DOPC lipid vesicles show that the results obtained with shaking can be highly misleading. Shown in Figure 24 (right panel), zwitterionic DOPC lipid vesicles were unable to trigger α-syn aggregation in PEGylated plates. When shaking in polystyrene plates, the presence of DOPC triggers α-syn aggregation (Figure 24, left panel). At higher lipid concentrations, above approximately 0.1 mM (L/P = 5), no aggregation is seen during the time frame of the experiment. At lower concentrations of DOPC, below approximately 0.1 mM, the aggregation of α-syn seems to occur at higher or similar rates as α-syn alone. One likely interpretation of these data is that the observed effects are linked to the deposition of a lipid film at the polystyrene surface. Meaning that at low lipid concentrations, interactions between the polystyrene surface and α-syn is similar to that of α-syn in the absence of DOPC lipid vesicles, generating nuclei through heterogeneous primary nucleation (Figure 15). At high concentrations of DOPC, the polystyrene surface may no longer be accessible to α-syn monomers, and therefore aggregation is not triggered. In order words, the observed effects can be due to blocking the surface-protein interactions rather than being due to lipid-protein interactions, and this example illustrates complications in interpreting data from various papers for a system that so strongly depends on the experimental conditions.

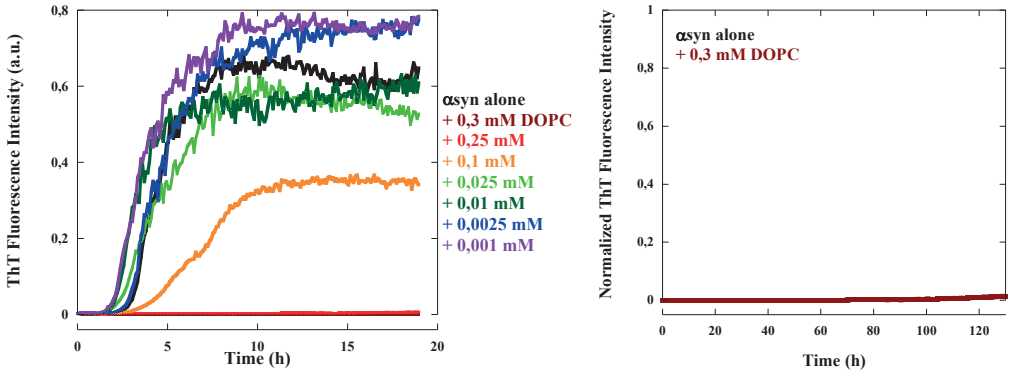

Figure 24. α-Syn aggregation in the presence of zwitterionic DOPC lipid vesicles. Aggregation kinetics of α-syn in the presence of zwitterionic DOPC vesicles was monitored by ThT at mildly acidic pH at 37°C **(left panel)** under shaking conditions in polystyrene plates and **(right panel)** under quiescent conditions in PEGylated plates. The figures show average traces of at least three experimental repeats (unpublished data).

4.7 How do biological membranes influence α-synuclein aggregation?

Prion-like propagation of misfolded α-syn was recently proposed as a key pathogenetic event in PD (110-116). In prion disease, misfolded protein spreads between cells, serving as templates triggering protein aggregation in the recipient cell. This hypothesis has gained great support, while the underlying molecular and cellular mechanisms are still not well understood. *In vitro* studies have implicated that the mechanisms underlying cell-to-cell transfer of α-syn involve exocytosis/endocytosis mechanisms (117-121). Exosomes, approximately 100 nm in size, are secreted vesicles into the extracellular space involved in cell-to-cell communication and have the ability to shuttle particular molecules. Recently, exosomes were suggested to be crucial to intercellular transfer of α-syn sequestrating and spreading pathological forms of α-syn (122-125).

It was shown in Paper IV that the aggregation of α-syn is accelerated by exosomes irrespective of whether derived from control cells (Figure 25) or cells overexpressing α-syn.

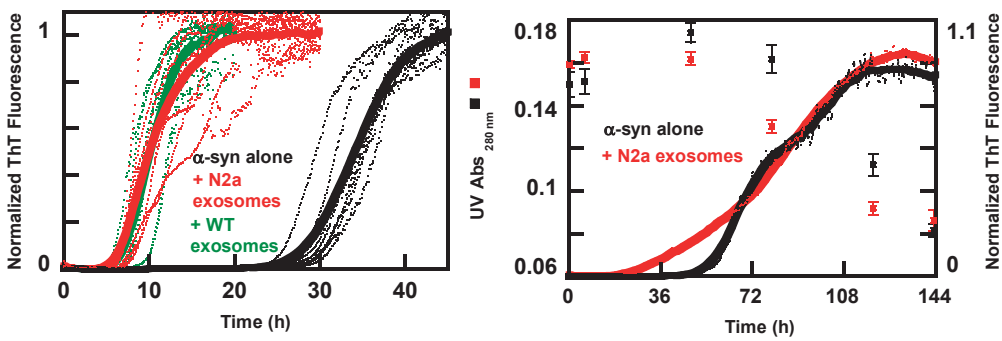

Figure 25. Aggregation kinetics of α-syn in the presence of exosomes. The aggregation kinetics of 30 μM α-syn was monitored by ThT in the presence and absence of exosomes in 10 mM MES buffer pH 5.5 with 140 mM NaCl. **Left panel,** aggregation of α-syn (black) with 0.25 mg/ml exosomes from N2a cells (red) or N2a cells overexpressing α-syn (green). Data collected at 100 rpm in polystyrene plates. The figure shows average traces in bold with dotted experimental repeats. **Right panel,** aggregation of α-syn (black line) in the presence of 0.25 mg/ml exosomes from N2a cells (red lines). Data collected under quiescent conditions in polystyrene plates. In parallel, the concentration of α-syn remaining in solution was measured by absorbance at 280 nm as a function of time (dotted points). The figure shows averages of at least three experimental repeats (Paper IV).

Lipid component responsible for catalytic nature

Vesicles composed of extracted exosome lipids were also catalytic implying that the lipid component is sufficient for this effect. Using mass spectrometry, several phospholipid species were identified, including PC, PS, PE and PI. Gangliosides GM2 and GM3, were also found to be components of exosomes. One should mention that for each lipid class, several species were identified with different acyl-chain lengths. Model lipid vesicles composed of ganglioside lipids, GM1 and GM3, (as GM2 is not commercially available) were shown to accelerate the aggregation in a concentration dependent manner, while other model lipid vesicles did not show such effect.

Conclusion:

Exosomes accelerate α-syn aggregation and this effect was shown to be due to the lipid composition, specifically gangliosides. Model membranes containing negatively or positively charged lipids were prepared to have similar charge densities as exosomes, however, none induced acceleration of the aggregation.

4.8 What lipid headgroup features drive α-synuclein association to lipid membranes?

The interactions between aggregating α-syn and lipid membranes will depend on the molecular properties of the system, including protein structure, net charge and charge distribution, as well as, solution conditions and membrane composition and phase behavior (Paper I, II, 67, 126-128). In order to understand what the important properties of the lipid system are one often uses model membranes where the lipid composition can be systematically varied.

α-Syn has been reported to associate with lipid rafts (129, 130), and ganglioside-containing membrane domains, including GM1 and GM3 (119, 131). This association of α-syn and gangliosides has been suggested to be due to a specific interaction between α-syn and both the sialic acid and sugar residues of gangliosides (119). Gangliosides are reported to be preferentially located in the outer leaflet of the plasma membrane. The recent hypothesis on cell-to-cell transmission suggests a role of extracellular α-syn in the spreading of the disease, meaning extracellular α-syn could interact with gangliosides located on the outer leaflet (132).

It was previously shown that GM-containing exosomes, as well as, vesicles prepared form extracted exosome lipids and ganglioside-containing model membranes accelerate α-syn aggregation. We therefore conducted a follow up study to understand whether the effects observed are related to specific interactions between α-syn and the ganglioside headgroup or if it is attributed to more generic properties of the lipid, such as, headgroup charge and size or lipid self-assembly (Paper V). The aggregation kinetic experiments were conducted at mildly acidic pH and low ionic strength (10 mM MES buffer pH 5.5) under quiescent conditions in non-binding PEGylated plates.

Effects of lipids on α-syn aggregation kinetics

To investigate the effect of lipid membranes on the aggregation of α-syn, model membranes composed of 90% zwitterionic DOPC and 10% anionic lipids, of GM1, GM3, DOPS or PE-PEG750 were used (Figure 26, Paper V). All these anionic lipid vesicles studied were shown to have a strong catalyzing effect on the aggregation of α-syn. One should highlight that all anionic lipid vesicles investigated displayed such accelerating effect. **In these experiments, the aggregation kinetics was studied at low ionic strength under quiescent conditions, which is different to the experimental conditions used in Paper IV.**

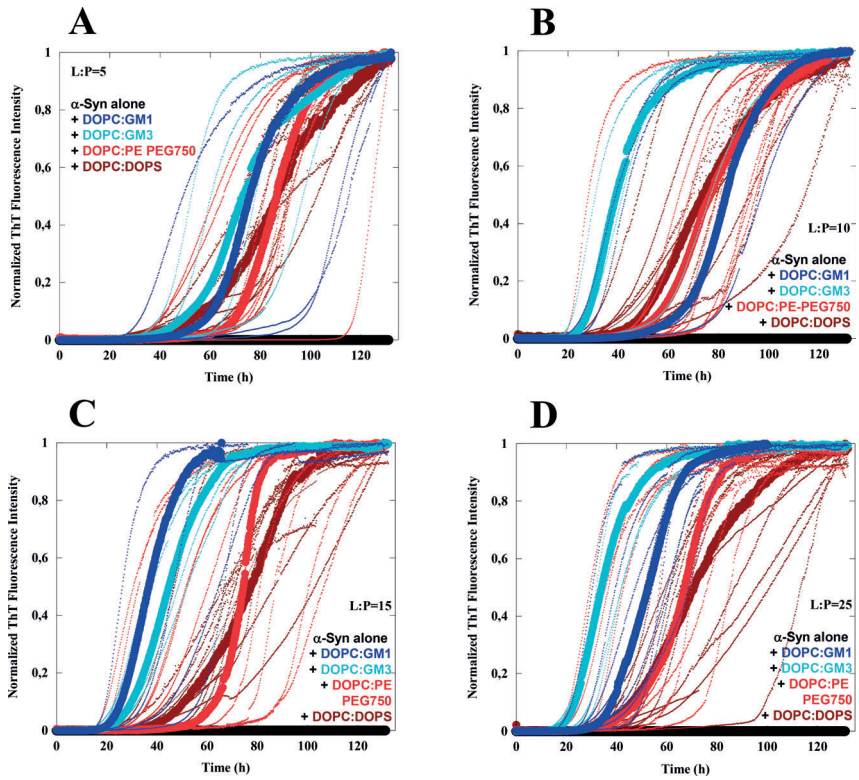

Figure 26. Aggregation kinetics of α-syn in the presence of anionic lipid membranes. The aggregation kinetics of 20 μM α-syn alone and in the presence of lipid vesicles at concentrations ranging from 0.1 to 0.5 mM was monitored by ThT at 37ºC under quiescent conditions. Median experimental traces are shown in bold with at least 5 experimental repeats dotted (Paper V).

Following the aggregation kinetics at low ionic strength and under quiescent conditions, it is observed a slightly more pronounced catalytic effect of gangliosides compared to other anionic lipid systems, at least for the higher lipid concentrations (Figure 26 and 27). Under such experimental conditions, α-syn alone and α-syn in the presence of zwitterionic DOPC lipid membranes does not aggregate up to several days (Paper V; Figure 24).

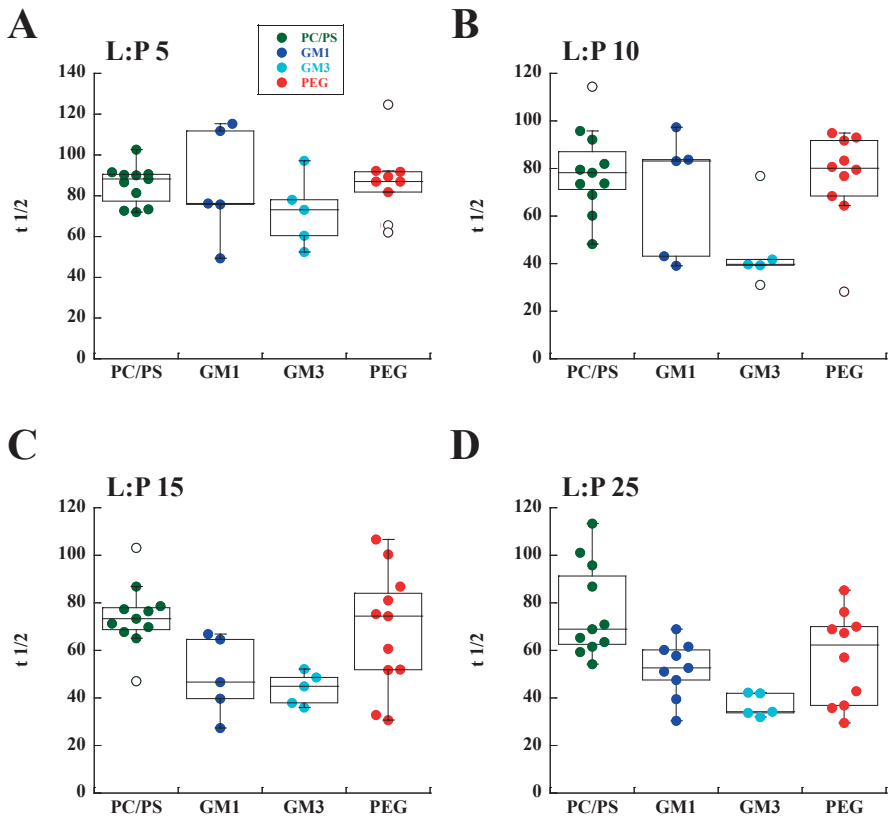

Figure 27. Aggregation kinetics of α-syn in the presence of anionic lipid membranes. The aggregation kinetics of 20 μM α-syn in the presence of anionic lipid vesicles at concentrations ranging from 0.1 to 0.5 mM was monitored by ThT at 37ºC under quiescent conditions. Statistical analysis is shown with both box and dot plots of all experimental repeats for each lipid concentration (unpublished data).

This catalytic effect of anionic lipid membranes seems to be dependent on the lipid-to-protein ratio. Meaning that, the aggregation kinetics is accelerated with increasing lipid concentration until a threshold is reached, were beyond that concentration the aggregation is progressively slowed down (Figure 28). At very high lipid-to-protein ratios aggregation is not observed (Figure 28). One possible explanation is that all peptide may be membrane-bound compatible with the observation of the need for excess monomer protein in solution for aggregation to be observable (Paper V; 54). α-Syn binding to these different anionic membranes was further studied and will be discussed in more detail below.

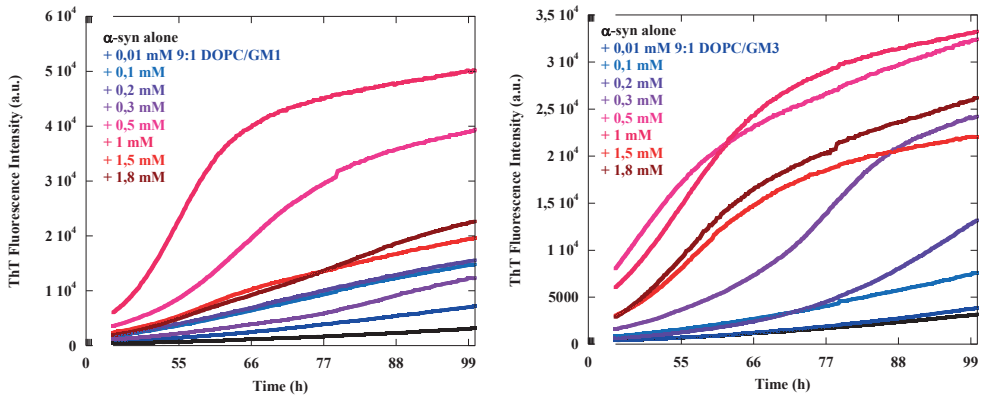

Figure 28. ThT aggregation kinetics of α-syn in the presence of ganglioside, both GM1 and GM3 containing lipid membranes. The aggregation kinetics of 20 μM of α-syn was monitored in the presence of 9:1 DOPC/GM1 (**left panel**) and 9:1 DOPC/GM3 (**right panel**) lipid vesicles with concentrations ranging from 0.01–1.8 mM, in nonbinding PEGylated plates under quiescent conditions at 37ºC in 10 mM MES buffer pH 5.5. The average traces of at least 3 experimental replicates are represented as solid lines (unpublished data).

How does α-syn adsorb to ganglioside-containing lipid bilayers

It has been reported that α-syn preferentially associates and adopts an α-helical conformation to membranes containing lipids with acidic headgroups, such as, PS, PG and PA (Paper IV and V, 54, 67, 128, 133). The adsorbed α-syn is located in the interfacial layer proximate to the lipid headgroups, and does not appear to penetrate deeply into the hydrophobic acyl-chain region of the membrane (134). This motivated the question, does α-syn bind in a similar manner to ganglioside-containing bilayers?

FCS was used to investigate peptide binding to lipid membranes by measuring peptide diffusion times. Fluorescently labeled α-syn was incubated with zwitterionic DOPC, DOPC/DOPS 9:1 and DOPC/GM1 9:1 lipid vesicles. The addition of zwitterionic DOPC had no or very little effect on the α-syn autocorrelation functions (diffusion times of labelled α-syn) at all lipid-to-protein ratios tested (Figure 29). This implies that protein mainly exists as a monomer in solution. Both DOPS and GM1 containing vesicles caused slower diffusion for α-syn at the higher lipid-to-protein ratios, implying that α-syn associates with anionic lipid membranes. The effects of both anionic lipid systems investigated were shown to be very similar (Figure 29).

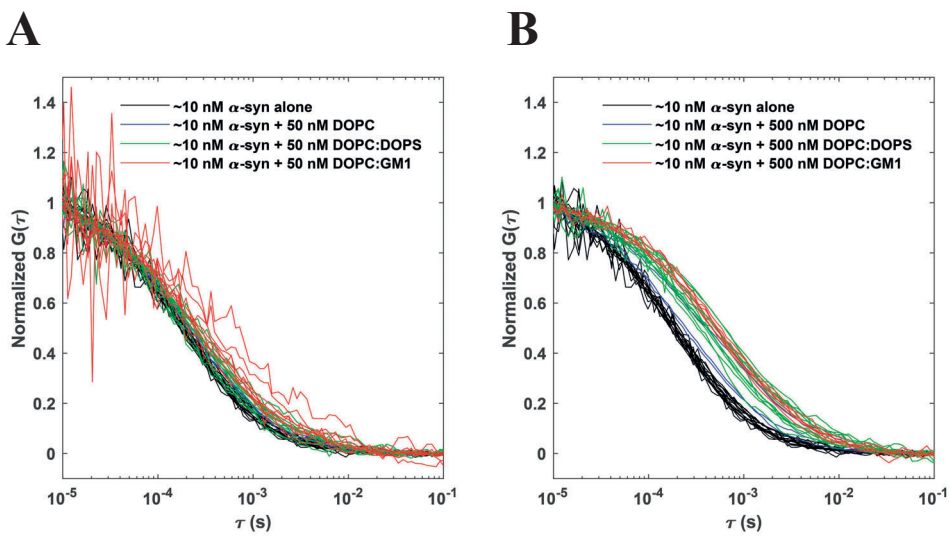

Figure 29. α-Syn relative binding affinity. 10 nM fluorescently labeled AF568-α-syn was incubated with pure DOPC (blue), 9:1 DOPC/DOPS (green) and 9:1 DOPC/GM1 (red) at different lipid-to-protein ratios. The normalized autocorrelation functions for the 3 different lipid systems are plotted for lipid-to-protein ratios 5 **(A)** and 50 **(B)** (unpublished data, experiments performed by Jon Pallbo and Aleksandra Dabkowska).

α-Syn structure upon association to lipid membranes

Protein structure upon lipid membrane binding was studied by ^{1}H-^{15}N-HSQC NMR and CD experiments. In sum, both two techniques reported similar results for DOPS and ganglioside-containing vesicles. The NMR experiments show that binding is taking place at the N-terminus, with the first 100 residues involved in the membrane-binding structure (Figure 30). CD studies demonstrate conformational change to α-helix (Paper V). For both systems the α-helicity signal observed by CD shared a very similar trend for the lipid-to-protein ratios investigated (Paper V).

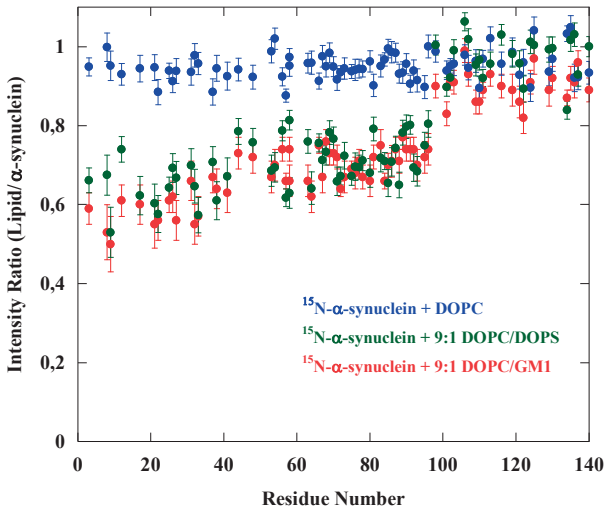

Figure 30. α-Syn conformation when associated to lipid membranes. Left panel) ^{1}H-^{15}N-HSQC spectra of 20 μM ^{15}N-α-syn were recorded in the absence and presence of 0.5 mM of each lipid system. The intensity ratios for each residue obtained from the ^{1}H-^{15}N-HSQC spectra are plotted for DOPC (blue), 9:1 DOPC/DOPS (green) and 9:1 DOPC/GM1 (red) (unpublished data).

Comparison between lipid headgroups of different charge and size

A set of experiments were designed to understand if the effects for ganglioside-containing membranes are related to specific interactions between α-syn and the ganglioside headgroup or if it is due to more generic properties of the lipid, such as, headgroup charge and size. The designed set of experiments intended to study both the influence on α-syn aggregation kinetics and conformational change upon interaction with lipids with different headgroups, such as Asialo-GM1 and PEGylated ceramide (structures shown in Figure 4). Both uncharged lipids, Asialo-GM1 and PEGylated ceramide were mixed with DOPC at a molar ratio of 9:1, analogous to the studies of anionic vesicles described above. In the presence of these lipid systems no α-syn α-helical conformational change was detected, however, quite unexpectedly aggregation was triggered even though the aggregation process was clearly slower compared to the situation where α-helical intermediates were formed in the presence of anionic lipid vesicles. This result implies that charge-independent interactions are also important for membrane-induced heterogeneous primary nucleation. It also suggests that α-helical α-syn intermediates are not required species in triggering aggregation, as previously proposed (91).

A short summary follows of the lipid systems investigated in terms of effect on

aggregation rate and conformational change (Paper V; Figure 31):

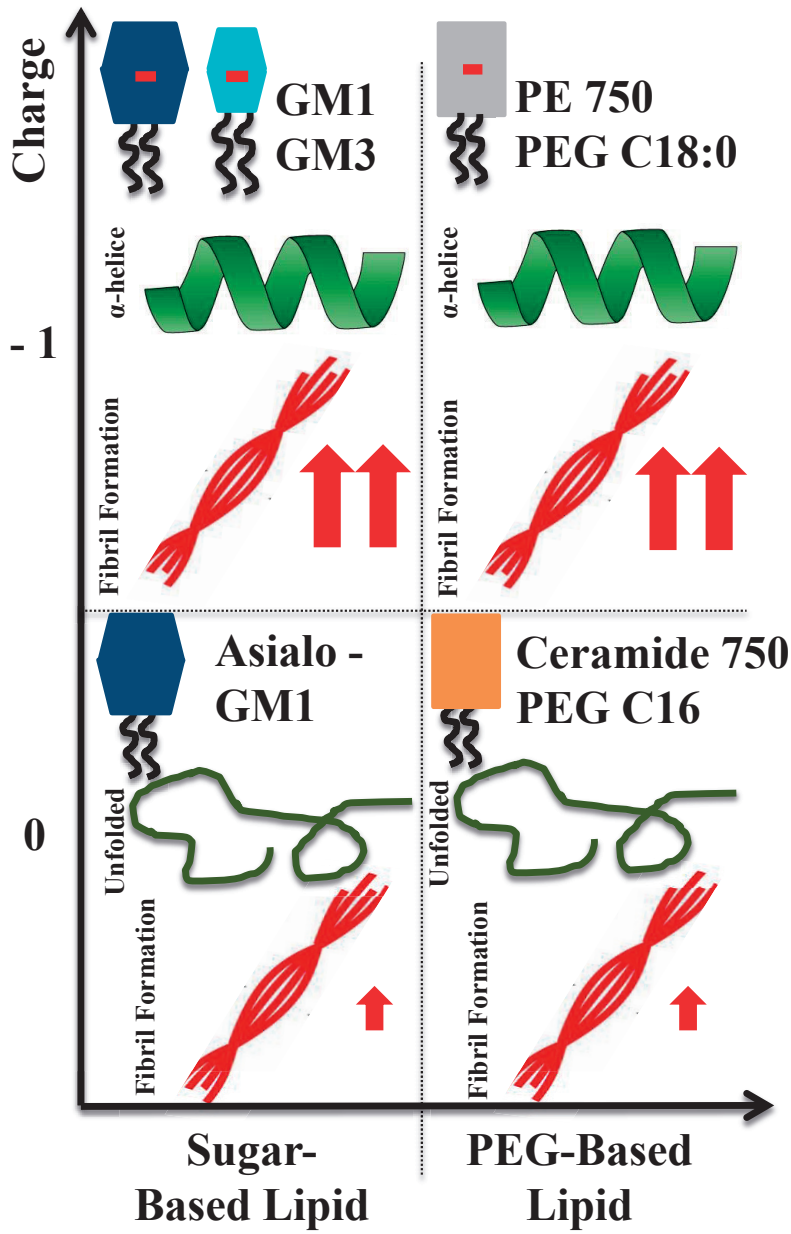

Figure 31. Summary of the results obtained for the aggregation kinetics and conformational change of α-syn in the presence of model membrane systems with different lipid compositions (Paper V).

Conclusion:

All anionic lipid systems investigated, GM1, GM3, DOPS and PE-PEG750 were shown to induce α-syn conformation change, from random coil to α-helix. The catalytic effect displayed by these anionic lipid vesicles on α-syn aggregation is due to enhancing heterogeneous primary nucleation (Figure 32; Paper V, VII, 54). The finding that a range of different lipid systems with relatively low content in anionic lipids trigger the aggregation process is very different from the observations reported at neutral pH where only certain lipid systems trigger α-syn aggregation (126).

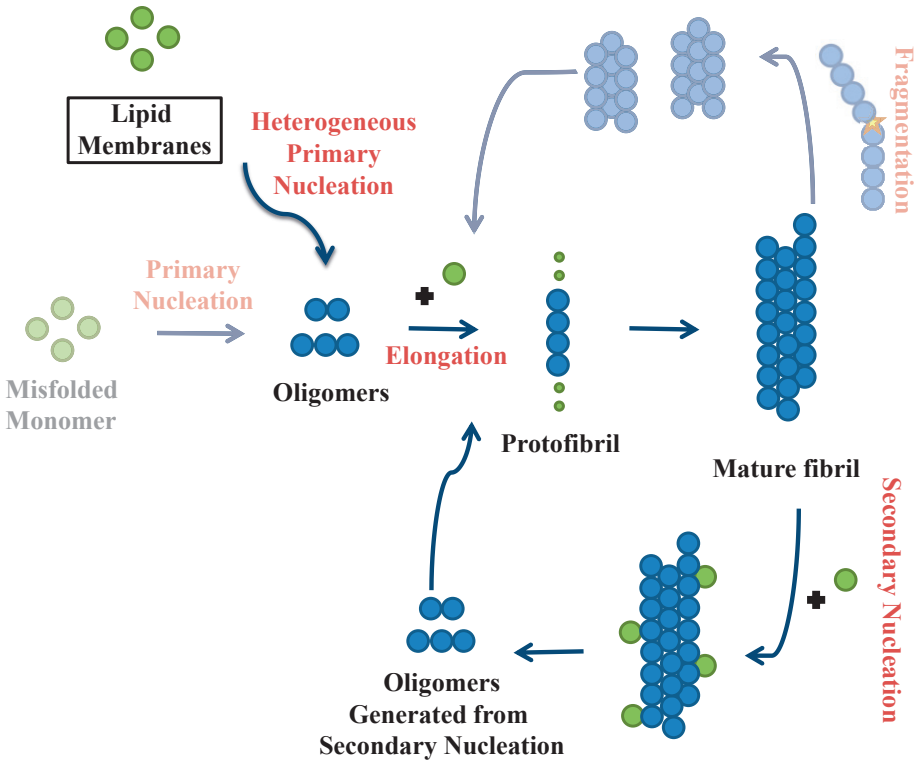

Figure 32: Anionic lipid membranes catalyse α-syn aggregation by enhancing heterogeneous primary nucleation. The microscopic events that are enhanced due to anionic lipid membranes are highlighted in the figure.

Investigating the catalytic effect of anionic lipid membranes on α-syn aggregation, it was shown that charge-based interactions induce conformational change of α-syn from random coil to α-helix and enhance aggregation kinetics. However,

charge-independent interactions are also important, as lipid membranes containing uncharged lipid species with large hydrophilic headgroups were shown to trigger α-syn aggregation, although far less efficiently and without inducing α-syn conformational change to α-helix.

A combined experimental approach showed that α-syn binding relative affinity and α-syn bound structure are similar between gangliosides and anionic lipid membranes investigated. However, the catalytic effect of ganglioside lipids on the aggregation of α-syn was shown to be somewhat greater than that of other anionic lipid membranes investigated in both high and low ionic strength solution conditions (Paper IV and Paper V). The molecular explanation for this difference in lipid-induced aggregation is still not fully understood.

4.9 Do lipids affect the morphology of the Protein-Lipid Co-aggregates?

We have investigated the structural evolution of α-syn aggregates formed in the presence of ganglioside-containing lipid vesicles imaging with cryo-TEM different time points along the aggregation reaction. As we have identified conditions for reproducible aggregation kinetics, it is possible to selectively take out samples and image these at different stages along the aggregation reaction (Figure 33):

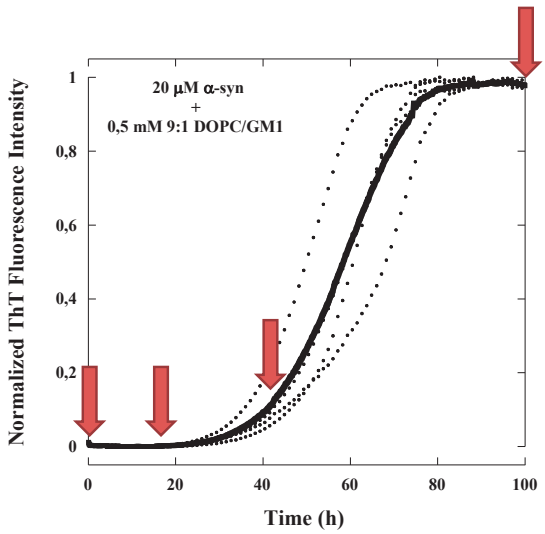

Figure 33. Aggregation kinetics of α-syn in the prescence of GM1 lipid vesicles. The aggregation kinetics of 20 μM α-syn in the presence of 0.5 mM DOPC/GM1 9:1 lipid vesicles was monitored using ThT at 37ºC under quiescent conditions. The average trace is shown in bold with experimental repeats dotted. Red arrows indicate the time points imaged with cryo-TEM (Paper VI).

Representative cryo-TEM images are shown in Figure 34 for each time point chosen to image:

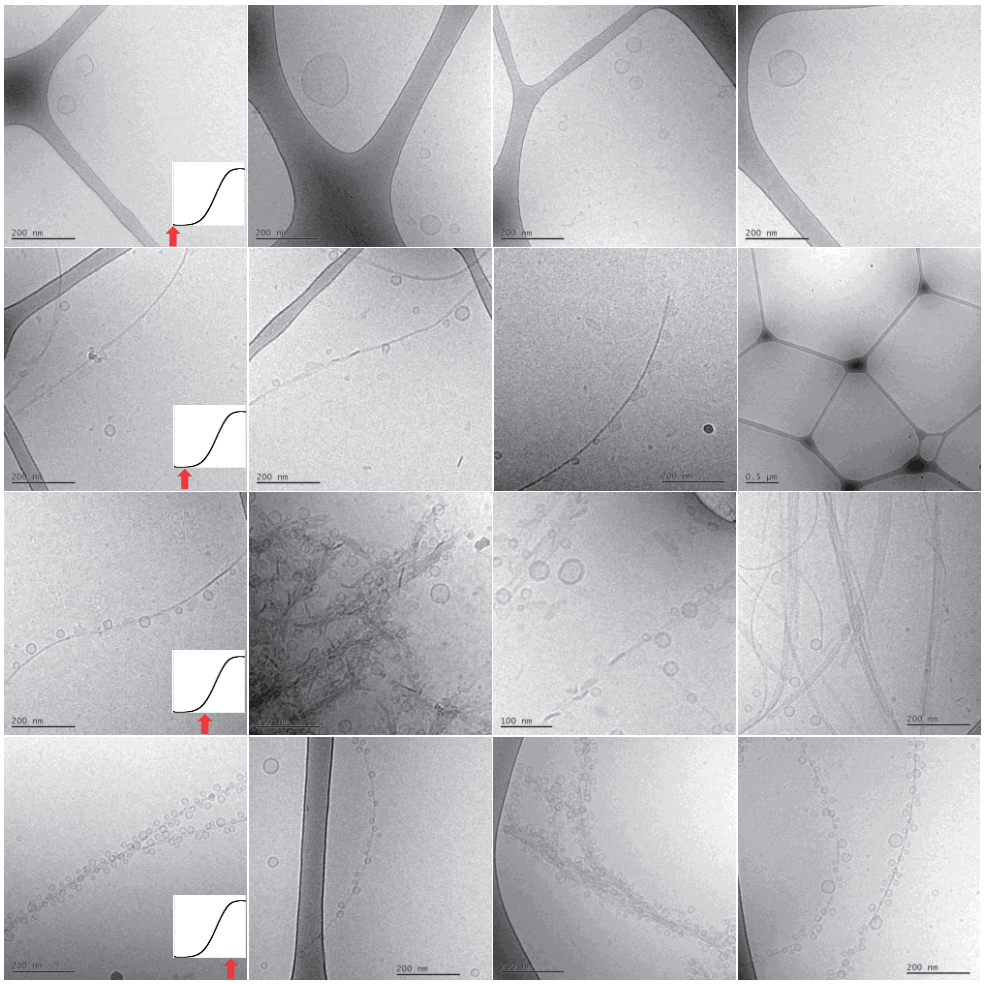

Figure 34. Imaging GM1 lipid vesicles in the presence of aggregating α-syn. Samples from different time points along the aggregation reaction (0h, 14h, 40h and plateau) were imaged on glow-discharged carbon grids (Paper VI).

Cryo-TEM allows us to verify that the morphology of α-syn-lipid co-aggregates are different when compared to aggregated protein alone (Figure 34 vs Figure 3, respectively). Looking at the cryo-TEM images interesting features can be observed (Figure 34). At time 0h, it seems that α-syn associates immediately with ganglioside membranes, causing the polydisperse population of vesicles to have irregular/non-spherical shapes (Top row). Sampling at the lag-phase, shows a significant decrease in the size distribution of the lipid vesicles, of which the smaller are mainly associated to fibrillar structures (Middle rows of Figure 34, Figure 35). Imaging at the end state (corresponding to the plateau in the kinetic

trace in Figure 33), the sample appeared to be more homogenous, with predominately long and curly fibrils decorated with small and very monodisperse lipid vesicles. Fibrils are also rather thin and dispersed rather than compact bundles, observed for fibrils of protein alone (Bottom row of Figure 34 vs Figure 3).

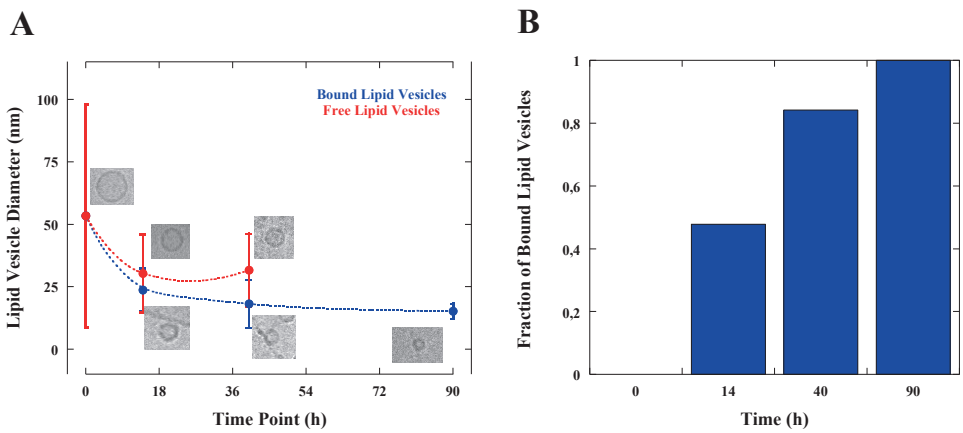

Figure 35. GM1 lipid vesicle size distribution as a function of time when in the presence of aggregating α-syn. (A) Representative lipid vesicles as a function of time along the aggregation reaction. The number of free lipid vesicles at time point 90 h is too low to get good statistics and therefore the corresponding data point is not added in the graph. **(B)** Fraction of number of bound lipid vesicles in relation to total number of lipid vesicles as a function of time (Paper VI).

Conclusion

Imaging α-synuclein-GM1 co-aggregation using cryo-TEM at different time points during the aggregation reaction revealed aggregates with different structural morphology compared to those formed from pure α-synuclein. The images also show a clear evolution of structures, and a dramatic decrease in vesicle size during the lagphase of the aggregation reaction (Paper VI).

Protein-lipid co-aggregation is expected to change the physical-chemical features of the aggregates. As surface properties may change due to the presence of lipids, it may also affect surface dependent mechanistic events in the aggregation process (Paper VI).

4.10 Are lipids taken up into amyloid aggregates during the co-aggregation process?

Co-localization of lipids and aggregated proteins has been demonstrated for some amyloid proteins using fluorescent lipid analogues (42, 109, 135). These studies demonstrate the presence of lipids in the aggregates, but provide no further molecular insight. The cryo-TEM studies in paper VI showed that lipids have an effect on fibril morphology. The morphology of the fibrils has also been shown to depend on the lipid system and lipid-to-protein ratio (74). Using model lipid systems of known composition, we explored whether lipid species are taken up during the aggregation process. The lipid systems investigated consisted of pure zwitterionic DOPC and mixtures of DOPC with different amounts of anionic DOPS. The total amount of co-aggregated phospholipids was determined by a quantitative phosphorous assay (Figure 36; 74). This method is easy and fast, although the sensitivity is low. Other methods with higher sensitivity, such as NMR and mass spectrometry, are being pursued as I write these results.

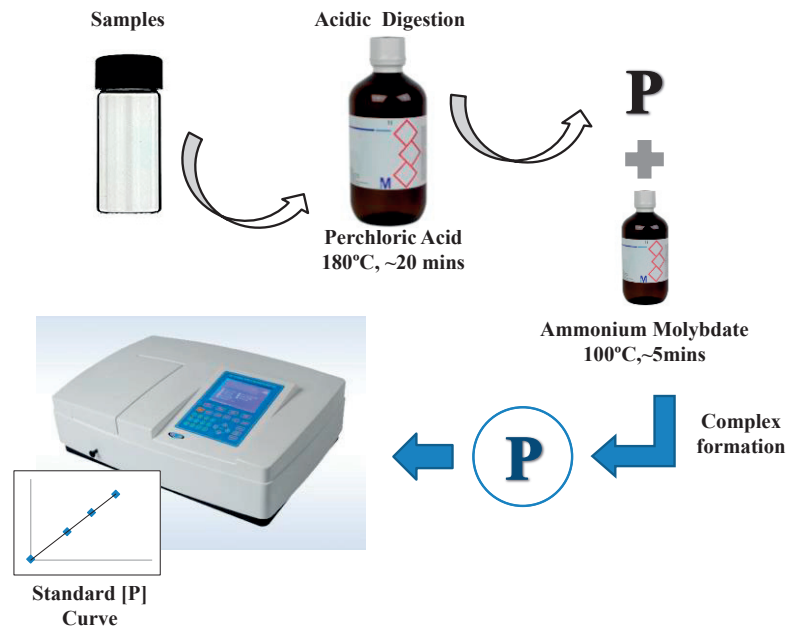

Figure 36. Schematic representation of the experimental protocol for the phosphorus assay.

To evaluate the effect of negative charge on lipid uptake during fibril formation, vesicles containing 0, 1, 10 and 30% anionic DOPS mixed with uncharged DOPC were incubated with α-syn (Figure 37).

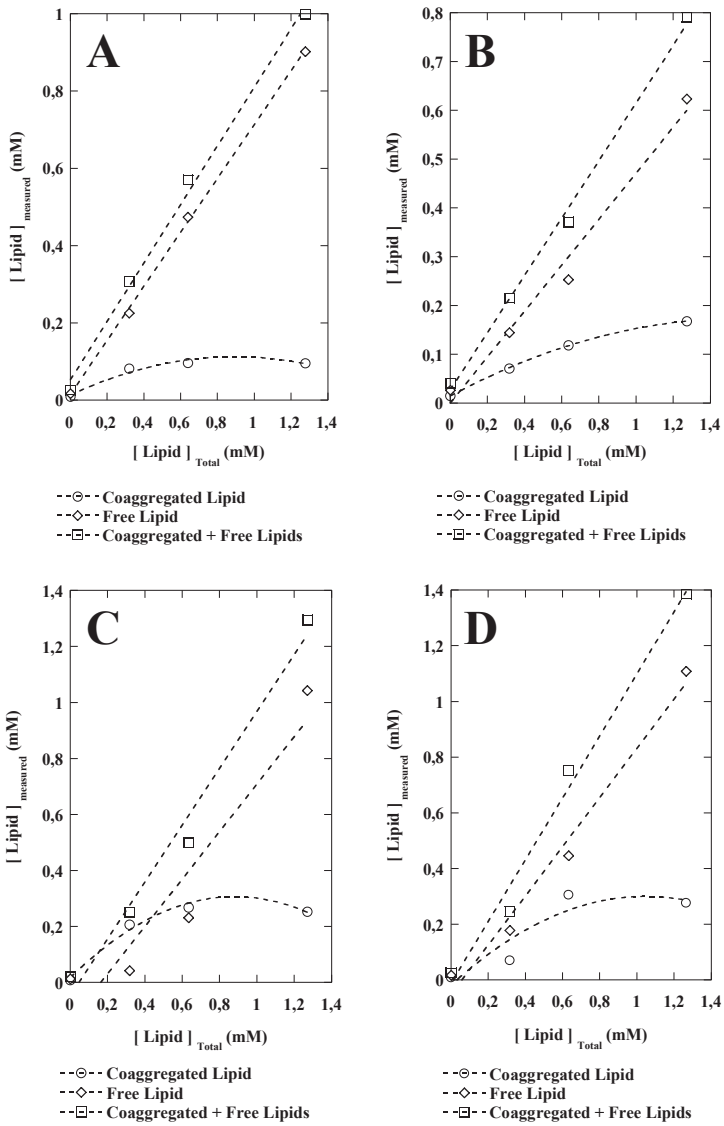

Figure 37. Lipid quantification in lipid-protein co-aggregates. Vesicles containing 0% **(A)**, 1% **(B)**, 10% **(C)** and 30% **(D)** anionic DOPS mixed with uncharged DOPC were incubated with α-syn overnight with shaking at 37ºC. Lipids present in the pellet of the samples were quantified using the phosphorus assay and shown as co-aggregated lipid in the figure (unpublished data).

Well depicted is the fact that increasing negative charge, by increasing the amount of DOPS in the DOPC-DOPS mixtures led to an increase in lipid uptake (co-aggregated lipid traces in Figure 37). In other words, the more DOPS the more co-aggregated lipid is present in the final aggregate. Even adding amounts as low as 1% DOPS leads to an increase in lipid uptake when compared to pure DOPC (Panel A *vs* B in Figure 37). One should highlight that the method does not distinguish between DOPC and DOPS. Two scenarios may be possible: the first being that lipid uptake can be selective to anionic lipids; the second being that the presence of anionic lipids are required for lipids to be taken up, but both charged and uncharged are then present in the final co-aggregate fibril.

Conclusion

Answering the question made in this chapter, lipids are taken up into the fibrillar structure during the aggregation process. The uptake process seems to be enhanced with the presence of anionic lipid species.

5.Outlook

Taking the thesis work altogether one can observe some overall trends combining results from different studies. Here, we have investigated α-syn aggregation for different solution conditions (varying pH and ionic strength) and also in the presence of different catalytic surfaces (of particular relevance are seeds and vesicles) enabling insights into nucleation. Whether this is nucleation of a monomer on the fibril surface of the same peptide, "secondary nucleation", or nucleation on a catalytic surface, such as, a lipid membrane, polystyrene surface, air-water interface or seeds of other peptides, "heterogeneous primary nucleation". The nucleation event may likely occur in a similar manner for some of these cases. This does not, however, mean that nucleation may not arise by other pathways, as suggested in Paper V. Following is an attempt to summarize some findings and proposing overall conclusions, some of which are speculations (in need of experiments to confirm):

1) The effect of α-syn seeds and anionic lipid vesicles was shown to trigger α-syn aggregation by enhancing nucleation (secondary nucleation in the case of seeds and heterogeneous primary nucleation in the case of lipid vesicles) at mildly acidic pH. This result suggests that different surfaces may have a similar effect on the aggregation of α-syn. In the case of anionic lipid vesicles, the catalytic ability is dependent on protein concentration. Meaning, excess monomer in solution is required for aggregation to be observed. Incoming α-syn in solution likely senses similar features when in the presence of both membrane-bound α-syn and α-syn incorporated in the fibrillar structure, which may consist of an extended unstructured α-syn C-terminal tail (Figure 38).

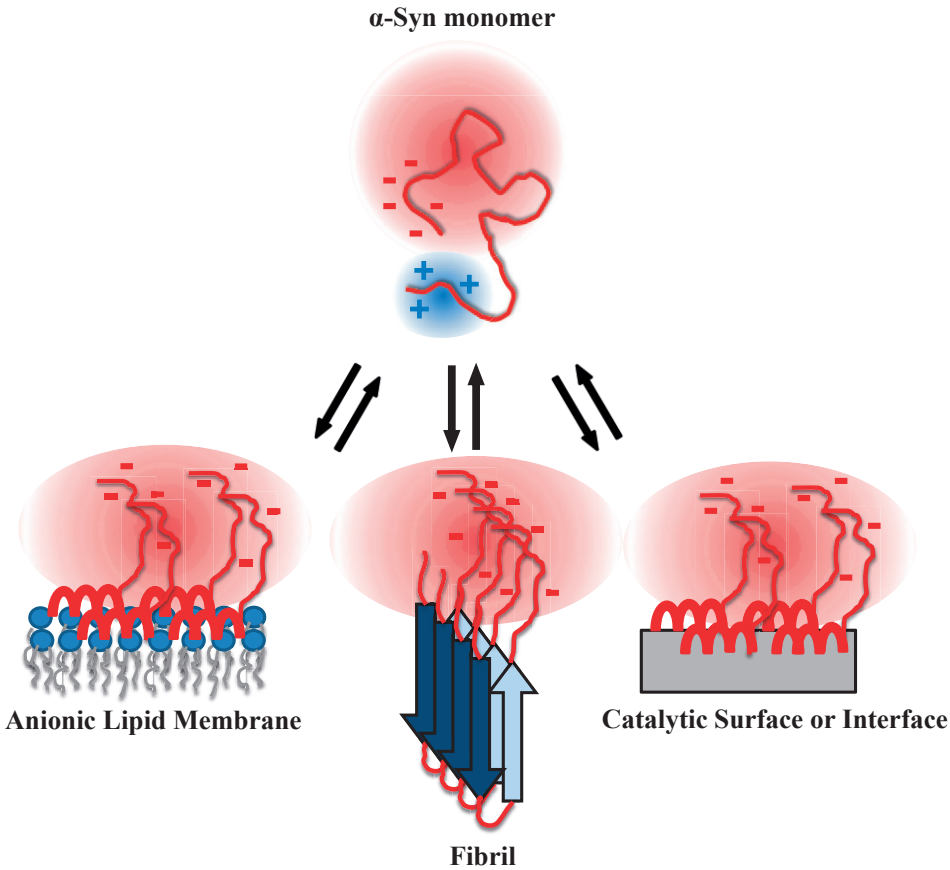

Figure 38. Schematic representation of what incoming α-syn senses in the case of membrane-bound α-syn or α-syn in a fibril or bound to a catalytic surface.

2) The effect of salt on α-syn aggregation was investigated both in the presence of catalytic seeds and anionic lipid vesicles at mildly acidic pH (Figure 39). Similar trends were again observed for both catalytic surfaces, were increasing ionic strength was shown to inhibit α-syn aggregation. One can postulate that interactions between the positively charged N-terminal regions of α-syn monomers and the negatively charged C-terminal tails of α-syn, decorating either fibrils or anionic vesicles, may be critical for nucleation (Figure 38). These attractive interactions between free and bound monomer would be screened by salt giving rise to the anomalous salt dependence of the aggregation observed (Figure 39).

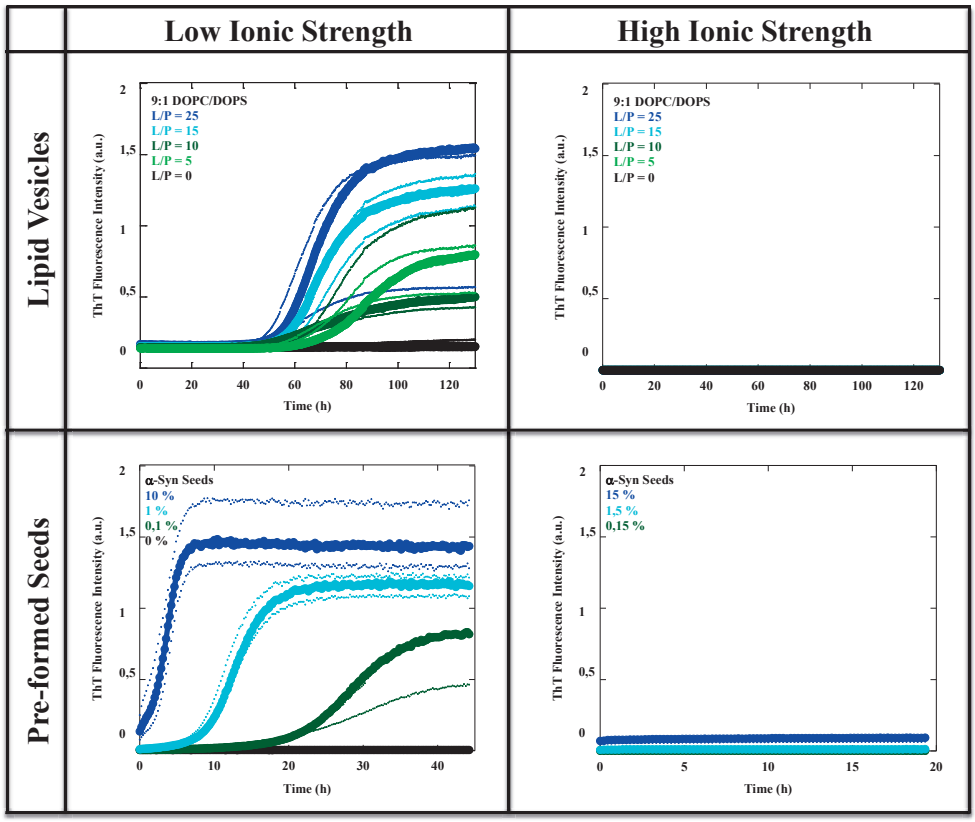

Figure 39. The effect of ionic strength on aggregation kinetics of α-syn in the presence of different catalytic surfaces. Aggregation kinetics of 20 μM α-syn monomer was monitored by ThT in the presence of two different catalytic surfaces, seeds and anionic lipid vesicles, in 10 mM MES buffer pH 5.5 at 37ºC under quiescent conditions without and with added 140 mM NaCl. The figure shows median traces in bold and at least three experimental repeats dotted (Paper VII).

3) The effect of pH on the aggregation of α-syn has also been investigated for both catalytic surfaces. At neutral pH, both types of catalytic surfaces do not display very strong effect on the aggregation of α-syn as compared to the situation of mildly acidic pH. In the case of lipid vesicles, at neutral pH only certain lipid systems purely composed of anionic lipids trigger α-syn aggregation (126). Increasing pH makes the N-terminal part of the protein less positively charged, and therefore less electrostatic attraction compared to mildly acidic conditions. This is consistent with the observation that at neutral pH lower amounts of α-syn bind to the anionic lipid systems here investigated when compared to mildly acidic pH. At neutral pH, aggregation of α-syn in the presence of α-syn seeds is observed. However, the aggregation mechanism is dominated by elongation through addition of monomeric α-syn. Monomer-dependent secondary nucleation

at neutral pH is undetectably slow. The reasoning is likely similar to that postulated above, less electrostatic attraction as a result of a less positively charged N-terminal region of α-syn.

A number of new questions arise from this PhD work, such as: Does nucleation happen at the surface? Does it involve free α-syn in transient interactions with bound α-syn? Does it take place in connection with the exchange process between bound α-syn and unbound relativelty unstructured α-syn? How large does the nuclei or oligomeric species grow before they detach?

6.References

(1) MA Gertz and SV Rajkumar (2010). Amyloidosis: Diagnosis and Treatment. Published by Springer ISBN:978-1-60761-6.
(2) CM Dobson (2003). Protein folding and misfolding. *Nature* 884-890.
(3) S Sambashivan and D Eisenberg (2006). Recent advances in decoding the structure of amyloid fibril. Published in BTi.
(4) DE Otzen (2013). Amyloid Fibrils and Prefibrillar Aggregates: Molecular and Biological Properties. Published by Wiley ISBN:9783527654208.
(5) KE Marshall and LC Serpell (2009). Insights into the Structure of Amyloid Fibrils. *The Open Biology Journal* 2:185-192.
(6) J Parkinson (1817). An Essay on the Shaking Palsy. Published by Sherwood, Neely and Jones.
(7) GE Alexander (2004). Biology of Parkinson´s disease: pathogenesis and pathophysiology of a multisystem neurodegenerative disorder. *Dialogues Clin. Neurosci.* 6(3): 259-280.
(8) WP Gai, HX Yuan, XQ Li, JT Power, PC Blumbergs and PH Jensen (2000). *In situ* and *In vitro* study of colocalization and segregation of α-synuclein, ubiquitin and lipids in Lewy bodies. *Exp. Neurol.* 166(2): 324-33.
(9) P Maiti, J Manna and GL Dunbar (2017). Current understanding of the molecular mechanism in Parkinson´s disease: Targets for potential treatments. *Translational Neurodegeneration* 6: 28.
(10) W Dauer and S Przedborski (2003). Parkinson´s Disease: Mechanisms and Models. *Neuron* 39(6): 889-909.
(11) AK Buell, C Galvagnion, R Gaspar, E Sparr, M Vendruscolo, TPJ Knowles, S Linse and CM Dobson (2014). Solution conditions determine the relative importance of nucleation and growth processes in α-synuclein aggregation. *PNAS U.S.A.* 111: 7671-7676.
(12) Methods in Enzymology: Amyloid, Prions and other protein aggregates (1999). Academic Press. Edited by Ronald Wetzel. Volume 309, ISBN: 9780121822101.
(13) FN Emamzadeh (2016). α-Synuclein structure, functions and interactions. *J. Res. Med. Sci.* 21: 29.
(14) J Burré (2015). The synaptic function of α-synuclein. *Journal of Parkinson´s Disease*. 5(4): 699-713.
(15) P Ibáñez, AM Bonnet, B Débarges, E Lohmann, F Tison, P Pollak, Y Agid, A Dürr and A Brice (2004). Causal relation between α-synuclein gene duplication and familial Parkinson´s disease. *Lancet*. 364(9440): 1169-71.
(16) E Masliah, E Rockenstein, I Veinbergs, M Mallory, M Hashimoto, A Takeda, Y Sagara, A Sisk and L Mucke (2000). Dopaminergic loss and inclusion body

formation in α-synuclein mice: implications for neurodegenerative disorders. *Science*. 287(5456): 1265-9.
(17) A Abeliovich, Y Schmitz, I Fariñas, D Choi-Lundberg, WH Ho, PE Castillo, N Shinsky, JM Verdugo, M Armanini, A Ryan, M Hynes, H Phillips, D Sulzer and A Rosenthal (2000). Mice lacking α-synuclein display functional deficits in the nigrostriatal dopamine system. *Neruon.* 25(1): 239-52.
(18) WS Davidson, A Jonas, DF Clayton and JM George (1998). Stabilization of α-synuclein secondary structure upon binding to synthetic membranes. *J. Biol. Chem*. 273: 9443-9449.
(19) D Eliezer, E Kutluay, R Bussell Jr and G Browne (2001). Conformational properties of α-synuclein in its free and lipid-associated states. *J. Mol. Biol.* 307: 1061-1073.
(20) N Lorenzen, L Lemminger, JN Pedersen, SB Nielsen and DE Otzen (2013). The N-terminus of α-synuclein is essential for both monomeric and oligomeric interactions with membranes. *FEBS Lett.* 588(3): 497-502.
(21) Y Atsmon-Raz and Y Miller (2016). Non-Amyloid-β component of human α-synuclein oligomers induces formation of new Aβ oligomers: Insight into the mechanims that link Parkinson´s and Alzheimer´s diseases. *ACS Chem. Neurosci.* 7(1): 46-55.
(22) H Han, PH Weinreb and PT Lansbury Jr (1995). The core Alzheimer´s peptide NAC forms amyloid fibrils which seed and are seeded by β-amyloid: Is NAC a common trigger or target in neurodegenerative disease? *Chemistry and Biology*. 2: 163-169.
(23) VN Uversky, J Li, P Souillac, IS Millett, S Doniach, R Jakes, M Goedert and AL Fink (2002). Biophysical properties of the synucleins and their propensity to fibrillate: Inibition of α-synuclein assembly by β- and γ-synucleins. *J. Biol. Chem*. 277(14): 11970-8.
(24) IM van der Wateren, TPJ Knowles, AK Buell, CM Dobson and C Galvagnion (2018). C-terminal truncation of α-synuclein promotes amyloid fibril amplification at physiological pH. *Chem. Sci*. doi:10.1039/C8SC01109E.
(25) K Levitan, D Chereau, SIA Cohen, TPJ Knowles, CM Dobson, AL Fink, JP Anderson, JM Goldstein and GL Millhauser (2016). Conserved C-terminal charge exerts a profound influence on the aggregation rate of α-synuclein. *J. Mol. Biol.* 411(2): 329-333.
(26) JD Sipe, MD Benson, JN Buxbaum, S Ikeda, G Merlini, MJM Saraiva and P Westermark (2010). Amyloid fibril protein nomenclature: 2010 recommendations from the nomenclature committee of the International Society of Amyloidosis. *Amyloid*. 17:3-4, 101-104.
(27) JM Squire, DAD Parry and AV Kajava (2006). Advances in Protein Chemistry. Fibrous Proteins: Amyloids, Prions and Beta Proteins. Published by Elsevier Academic Press ISBN:10:0-12-034273-1.

(28) BH Toyama and JS Welssman (2011). Amyloid Structure: Conformational diversity and consequences. *Annu. Rev. Biochem.* 80: 557-85.
(29) JL Jiménez, EJ Nettleton, M Bouchard, CV Robinson, CM Dobson and HR Saibil (2002). The protofilament structure of insulin amyloid fibrils. *PNAS U.S.A.* 99(14): 9196-9201.
(30) F Chiti and CM Dobson (2006). Protein misfolding, functional amyloid and human disease. *Annu. Rev. Biochem.* 75: 333-366.
(31) M Schleeger, CC van der Akker, T Deckert-Gaudig, V Deckert, KP Velikov, G Koenderink and M Bonn (2013). Amyloids: From molecular structure to mechanical properties. *Polymer* 54(10): 2473-2488.
(32) CM Dobson (1999). Protein misfolding, evolution and disease. *Trends in Biochemical Sciences* 24(9): 329-332.
(33) J Greenwalg and R Riek (2010). Biology of Amyloid: Structure, function and regulation. *Structure*. 18(10): 1244-60.
(34) AJ Geddes, KD Parker, ED Atkins and E Beighton (1968). Cross-beta conformation in proteins. *J. Mol. Biol*. 32(2): 343-58.
(35) KW Tipping, TK Karamanos, T Jakhria, MG Iadanza, SC Goodchild, R Tuma, NA Ranson, EW Hewitt and SE Radford (2015). pH-induced molecular shedding drives the formation of amyloid fibril-derived oligomers. *PNAS* USA 112(18): 5691-5696.
(36) R Gaspar, G Meisl, AK Buell, L Young, CF Kaminski, TPJ Knowles, E Sparr and S Linse (2017). Secondary nucleation of monomers on fibril surface dominates α-synuclein aggregation and provides autocatalytic amyloid amplification. *Quarterly Reviews of Biophysics.* 50(e6): 1-12.
(37) SIA Cohen, S Linse, LM Luheshi, E Hellstrand, DA White, L Rajah, DE Otzen, M Vendruscolo, CM Dobson and TPJ Knowles (2013). Proliferation of amyloid-beta 42 aggregates occurs through secondary nucleation mechanism. *PNAS U.S.A.* 110: 9758-9763.
(38) L Pieri, K Madiona, L Bousset and R Melki (2012). Fibrillar α-synuclein and huntingtin exon 1 assemblies are toxic to the cells. *Biophys. J.* 102(12): 2894-2905.
(39) N Cremades, SIA Cohen, E Deas, AY Abramov, AY Chen, A Orte, M Sandal, RW Clarke, P Dunne, FA Aprile, CW Bertoncini, NW Wood, TPJ Knowles, CM Dobson and D Klenerman (2012). Direct observation of the interconversion of normal and toxic forms of α-synuclein. *Cell* 149(5): 1048-1059.
(40) H Olzscha, SM Schermann, AC Woerner, S Pinkert, MH Hecht, GG Tartaglia, M Vendruscolo, M Hayer-Harti, FU Harti and RM Vabulas (2011). Amyloid-like aggregates sequester numerous metastable proteins with essential cellular functions. *Cell* 144(1): 67-78.
(41) SW Chen, S Drakulic, E Deas, M Ouberai, FA Aprile, R Arranz, S Ness, C Roodveldt, T Guilliams, EJ De-Genst, D Klenerman, NW Wood, TPJ Knowles, C Afonso, G Rivas, AY Abramov, JM Valpuesta, CM Dobson and N Cremades

(2015). Structural characterization of toxic oligomers that are kinetically trapped during α-synuclein fibril formation. *PNAS* USA 112(16): E1994-E2003.
(42) E Sparr, MF Engel, DV Sakharov, M Sprong, J Jacobs, B de Kruijff, JW Höppener and JA Killian (2004). Islet amyloid polypeptide-induced membrane leakage involves uptake of lipids by forming amyloid fibers. *FEBS Lett.* 577(1-2): 177-20.
(43) R Kayed, E Head, JL Thompson, TM McIntire, SC Milton, CW Cotman and CG Glabe (2003). Common structure of soluble amyloid oligomers implies common mechanism of pathogenesis. *Science* 300(5618): 486-9.
(44) F Oosawa, S Asakura, K Hotta, I Nobuhisa, T Ooi (1959). G-F transformation of actin as a fibrous condensation. *J. Polym. Sci.* 323-336.
(45) FA Ferrone, J Hofrichter, HR Sunshine, WA Eaton (1980). Kinetic studies on photolysis-induced gelation of sickle cell hemoglobin suggest a new mechanism. *Biophys. J.* 32: 361-377.
(46) SIA Cohen, M Vendruscolo, CM Dobson and TPJ Knowles (2012). From macroscopic measurements to microscopic mechanisms of protein aggregation. *J. Mol. Biol.* 421: 160-171.
(47) S Linse (2017). Monomer-dependent secondary nucleation in amyloid formation. *Biophys. Rev.* 9(4): 329-338.
(48) P Arosio, TPJ Knowles and S Linse (2015). On the lag phase in amyloid fibril formation. *Phys. Chem. Chem. Phys.* 17: 7606.
(49) R Khurana, C Coleman, C Ionescu-Zanetti, SA Carter, V Krishna, RK Grover, R Roy and S Singh (2005). Mechanism of Thioflavin T binding to amyloid fibrils. *Journal of Structural Biology.* 151: 229-238.
(50) SA Hudson, H Ecroyd, TW Kee and JA Carver (2009). The thioflavin T fluorescence assay for amyloid fibril detection can be biased by the presence of exogenous compounds. *FEBS Journal.* 276: 5960-5972.
(51) MRH Krebs, EHC Bromley and AM Donald (2004). The binding of thioflavin-T to amyloid fibrils: localization and implications. *Journal of Structural Biology.* 149: 30-37.
(52) C Xue, TY Lin, D Chang and Z Guo (2017). Thioflavin T as an amyloid dye: fibril quantification, optimal concentration and effect on aggregation. *R. Soc. open sci.* 4: 160696.
(53) G Meisl, JB Kirkegaard, P Arosio, TC Michaels, M Vendruscolo, CM Dobson, S Linse and TP Knowles (2016). Molecular mechanisms of protein aggregation from global fitting of kinetic models. *Nat. Protoc.* 11(2): 252-72.
(54) C Galvagnion, AK Buell, G Meisl, TCT Michaels, M Vendruscolo, TPJ Knowles and CM Dobson (2015). Lipid vesicles trigger α-synuclein aggregation by stimulating primary nucleation. *Nat. Chem. Biol.* 11, 229-234.
(55) M Kranenburg and B Smit (2005). Phase behavior of model lipid bilayers. *J. Phys. Chem. B.* 109: 6553-6563.

(56) FA Herberle and GW Feigenson (2011). Phase separation in lipid membranes. *Cold Spring Harb. Perspect. Biol.* 3(4).
(57) DM Engelman (2005). Membranes are more mosaic than fluid. *Nature* 438.
(58) G van Meer, DR Voelker and GW Feigenson (2008). Membrane lipids: where they are and how they behave. *Nat. Rev. Mol. Cell Biol.* 9(2): 112-124.
(59) PA Janmey and PKJ Kinnunen (2006). Biophysical properties of lipids and dynamic membranes. *TRENDS in Cell Biology.* 16(10): 538-46.
(60) J Fantini, N Garmy, R Mahfoud and N Yahi (2002). Lipid rafts: structure, function and role in HIV, Alzheimer´s and prion diseases. *Expert Rev. Mol. Med.* 4(27): 1-22.
(61) K Simon and E Ikonen (1997). Functional rafts in cell membranes. *Nature.* 387: 569-572.
(62) RJ Perrin, WS Woods, DF Clayton and JM George (2000). Interaction of Human α-synuclein and Parkinson´s disease variants with phospholipids. *J. Biol. Chem.* 275(44): 34393-34398.
(63) B Nuscher, F Kamp, T Mehnert, S Odoy, C Haass, PJ Kahle and K Beyer (2004). α-synuclein has a high affinity for packing defects in a bilayer membrane. *J. Biol. Chem*. 279(21): 21966-21975.
(64) L Milanesi, T Sheynis, W Xue, EV Orlova, AL Hellewell, R Jelinek, EW Hewitt, SE Radford and HR Saibil (2012). Direct three-dimensional visualization of membrane disruption by amyloid fibrils. *PNAS U.S.A*. 109(50): 20455-20460.
(65) HA Lashuel, D Hartley, BM Petre, T Walz and PT Lansbury Jr (2002). Neurodegenerative disease: amyloid pores from pathogenic mutations. *Nature.* 418: 291.
(66) K Furukawa, M Matsuzaki-Kobayashi, T Hasegawa, A Kikuchi, N Sugeno, Y Itoyama, Y Wang, PJ Yao, I Bushlin and A Takeda (2006). Plasma membrane ion permeability induced by mutant α-synuclein contributes to the degeneration of neural cells. *J. Neurochem.* 97: 1071-1077.
(67) BD van Rooijen, MMAE Claessens and V Subramaniam (2009). Lipid bilayer disruption by oligomeric α-synuclein depends on bilayer accessibility of the hydrophobic core. *Biochimica et Biophysica Acta.* 1788: 1271-1278.
(68) WS Davidson, A Jonas, DF Clayton and JM George (1998). Stabilization of α-synuclein secondary structure upon binding to synthetic membranes. *Journal of Biological Chemistry*. 273(16): 9443-9449.
(69) M Grey, CJ Dunning, R Gaspar, C Grey, P Brundin, E Sparr and S Linse (2015). Exosomes accelerate α-synuclein aggregation. *Journal of Biological Chemistry* 290(5): 2969-2982.
(70) GP Gorbenko and PK Kinnunen (2006). The role of lipid-protein interactions in amyloid-type protein fibril formation. *Chem. Phys. Lipids.* 141(1-2): 72-82.
(71) GP Gellermann, TR Appel, A Tannert, A Radestock, P Hortschansky, V Schroeckh, C Leisner, T Lütkepohl, S Shtrasburg, C Röcken, M Pras, RP Linke, S

Diekmann and M Fändrich (2005). Raft lipids as common components of human extracellular amyloid fibrils. *PNAS U.S.A.* 102: 6297–6302.
(72) C Cecchi, D Nichino, M Zampagni, C Bernacchioni, E Evangelisti, A Pensalfini, G Liguri, A Gliozzi and M Stefani (2009). A protective role for lipid raft cholesterol against amyloid-induced membrane damage in human neuroblastoma cells. *Biochim. Biophys*. *Acta.* 1788: 2204–2216.
(73) S Subasinghe, S Unabia, CJ Barrow, SS Mok, MI Aguilar and DH Small (2003). Cholesterol is necessary both for the toxic effect of Abeta peptides on vascular smooth muscle cells and for Aβ binding to vascular smooth muscle cell membranes. *J. Neurochem*. 84: 471–479.
(74) E Hellstrand, A Nowacka, D Topgaard, S Linse and E Sparr (2013). Membrane lipid co-aggregation with α-synuclein fibrils. *PloS ONE*. 8(10): e77235.
(75) GM Halliday, A Ophof, M Broe, PH Jensen, E Kettle, H Fedorow, MI Cartwright, FM Griffiths, CE Shepherd and KL Double (2005). α-Synuclein redistributes to neuromelanin lipid in the substantia nigra early in Parkinson´s disease. *Brain.* 128: 2654-2664.
(76) YA Domanov and PK Kinnunen (2008). Islet amyloid polypeptide forms rigid lipid-protein amyloid fibrils on supported phospholipid bilayers. *J. Mol. Biol.* 376(1): 42-54.
(77) A van Maarschalkerweerd, V Vetri, AE Langkilde, V Foderà and B Vestergaard (2014). Protein/lipid coaggregates are formed during α-Synuclein-induced disruption of lipid bilayers. *Biomacromolecules.* 15(10): 3643-3654.
(78) J Kiskis, H Fink, L Nyberg, J Thyr, J Li, A Enejder (2015). Plaque-associated lipids in Alzheimer´s diseased brain tissue visualized by nonlinear microscopy. *Scientific Reports*. 5: 13489.
(79) K Sasahara, K Morigaki and Y Mori (2015) Uptake of raft components into amyloid β-peptide aggregates and membrane damage. *Analytical Biochemistry*. 481: 18-26.
(80) NP Reynolds, A Soragni, M Rabe, D Verdes, E Liverani, S Handschin, R Riek and S Seeger (2011). Mechanism of membrane interaction and disruption by α-synuclein. *J. Am. Chem. Soc.* 133(48): 19366-75.
(81) Z Niu, W Zhao, Z Zhang, F Xiao, X Tang and J Yang (2014). The molecular structure of Alzheimer β-amyloid fibrils formed in the presence of phospholipid vesicles. *Angew. Chem. Inte. Ed. Engl.* 53(35): 9294-7.
(82) C Eichmann, S Bibow and R Riek (2017). α-Synuclein lipoprotein nanoparticles. *Nanotechnology Reviews* 6(1): 105-110.
(83) C Eichmann, S Campioni, J Kowal, I Maslennikov, J Gerez, X Liu, J Verasdonck, N Nespovitaya, S Choe, B Meier, P Picotti, J Rizo, H Stahlberg and R Riek (2016). Preparation and characterization of stable α-Synuclein lipoprotein particles. *The Journal of Biological Chemistry* 291(16): 8516-8527.

(84) Y Sui, KM Bullock, MA Erickson, J Zhang and WA Banks (2015). Alpha Synuclein is transported into and out of the brain by the blood-brain barrier. *Peptides* 62: 197-202.
(85) A Surguchov (2017). Commentary: α-Synuclein interacts with lipoproteins in plasma. *Front. Mol. Neurosci.* 10:362.
(86) WD McCubbin, CM Kay, S Narindrasorasak and R Kisilevsky (1988). Circular-dichroism studies on two murine serum amyloid A proteins. *Biochem. J.* 256: 775-783.
(87) M Gasset, MA Baldwin, RJ Fletterick and SB Prusiner (1993). Perturbations of the secondary structure of the scrapie prion protein under conditions that alter infectivity. *PNAS U.S.A.* 90: 1-5.
(88) N Cho, CW Frank, B Kasemo and F Höök (2010). Quartz crystal microbalance with dissipation monitoring of supported lipid bilayers on various substrates. *Nature Protocols* 5(6): 1096-1106.
(89) G Dunér, E Thormann and A Dėdinaitė (2013). Quartz crystal microbalance with dissipation (QCM-D) studies of the viscoelastic response from a continuously growning grafted polyelectrolyte layer. *Journal of Colloid and Interface Science* 408: 229-234.
(90) S Campioni, G Carret, S Jordens, L Nicoud, R Mezzenga and R Riek (2014). The presence of an air-water interface affects formation and elongation of α-synuclein fibrils. *JACS* 136: 2866-2875.
(91) VN Uversky, J Li and AL Fink (2001). Evidence for a partially folded intermediate in α-synuclein formation. *Journal of Biological Chemistry* 276: 10737-10744.
(92) LA Munishkina, J Henriques, VN Uversky and AL Fink (2004). Role of protein-water interactions and electrostatics in α-synuclein fibril formation. *Biochemistry* 43: 3289-3300.
(93) B Ashmad, Y Chen and LJ Lapidus (2012). Aggregation of α-synuclein is kinetically controlled by intramolecular diffusion. *PNAS* USA. 109: 2336-2341.
(94) R Vácha, S Linse and M Lund (2014). Surface effects on aggregation kinetics of amyloidogenic peptides. *JACS*. 136: 11776-11782.
(95) C Wang, N Shah, G Thakur, F Zhou and RM Leblanc (2010). α-Synuclein in α-helical conformation at air-water interface: implication of conformation and orientation changes during its accumulation/aggregation. *Chem. Commun. (Camb)* 46(36): 6702-4.
(96) D Pinotsi, AK Buell, C Galvagnion, CM Dobson, GSK Schierle and CF Kaminski (2014). Direct observation of heterogeneous amyloid fibril growth kinetics via two-color super-resolution microscopy. *Nano. letters.* 14: 339-345.
(97) A Abelein, J Jarvet, A Barth, A Gräslund and J Danielsson (2016). Ionic strength modulation of the free energy landscape of Aβ40 peptide fibril formation. *J. Am. Chem. Soc*. 138: 6893-6902.

(98) G Meisl, X Yang, CM Dobson, S Linse and TPJ Knowles (2017). Modulation of electrostatic interactions to reveal a reaction network unifying the aggregation behavior of the Aβ42 peptide and its variants. *Chem. Sci*. 8(6): 4352-4362.
(99) C Månsson, RTP van Cruchten, U Weininger, X Yang, R Cukalevski, P Arosio, CM Dobson, TPJ Knowles, M Akke, S Linse and C Emanuelsson (2018). Conserved S/T-residues of the human chaperone DNAJB6 are required for effective inhibition of Aβ42 amyloid fibril. *Biochemistry* (ahead of print).
(100) FA Aprile, P Arosio, G Fusco, SW Chen, JR Kumita, A Dhulesia, P Tortora, TPJ Knowles, M Vendruscolo, CM Dobson and N Cremades (2017). Inhibition of α-synuclein fibril elongation by HSP70 is governed by a kinetic binding competition between α-synuclein species. *Biochemistry* 56(9): 1177-1180.
(101) P Arosio, TC Michaels, S Linse, C Månsson, C Emanuelsson, J Presto, J Johansson, M Vendruscolo, CM Dobson and TPJ Knowles (2016). Kinetic analysis reveals the diversity of microscopic mechanisms through which molecular chaperones suppress amyloid formation. *Nat. Commun*. 7:10948.
(102) SIA Cohen, P Arosio, J Presto, FR Kurudenkandy, H Biverstal, L Dolfe, C Dunning, X Yang, B Frohm, M Vendruscolo, J Johansson, CM Dobson, A Fisahn, TPJ Knowles and S Linse (2015). A molecular chaperone breaks the catalytic cycle that generated toxic Aβ oligomers. *Nat. Struct. Mol. Biol.* 22(3): 207-213.
(103) V Kakkar, C Månsson, EP de Mattos, S Bergink, M van der Zwaag, MAWH van Waarde, NJ Kloosterhius, R Melki, RTP van Cruchten, S Al-Karadaghi, P Arosio, CM Dobson, TPJ Knowles, GP Bates, JM van Deursen, S Linse, B van de Sluis, C Emanuelsson and HH Kampinga (2016). The S/T-rich motif in the DNAJB6 chaperone delays polyglutamine aggregation and the onset of disease in a mouse model. *Mol. Cell*. 62(2): 272-283.
(104) CA Waudby, TPJ Knowles, GL Devlin, JN Skepper, H Ecroyd, JA Carver, ME Welland, J Christodoulou, CM Dobson and S Meehan (2010). The interaction of αB-crystallin with mature α-synuclein amyloid fibrils inhibits their elongation. *Biophysical Journal* 98: 843-851.
(105) CM Sax and J Piatigorsky (1994). Expression of the α-crystallin/ small heat-shock protein/ molecular chaperone genes in the lens and other tissues. *Adv. Enzymol. Relat. Areas Mol. Biol.* 69: 155-201.
(106) DM Hatters, RA Lindner, JA Carver and GJ Howlett (2001). The molecular chaperone, α-Crystallin, inhibits amyloid formation by apolipoprotein C-II. *The Journal of Biological Chemistry*. 276(36): 33755-33761.
(107) E Hellstrand, B Boland, DM Walsh and S Linse (2010). Amyloid β-Protein aggregation produces highly reproducible kinetic data and occurs by a two-phase process. *ACS Chem. Neurosci.* 1(1): 13-18.
(108) E Hellstrand, E Sparr and S Linse (2010). Retardation of Aβ fibril formation by phospholipid vesicles depends on membrane phase behaviour. *Biophys. J.* 98(10): 2206-2214.

(109) M Grey, S Linse, H Nilsson, P Brundin and E Sparr (2011). Membrane interaction of α-synuclein in different aggregation states. *J.P.D*. 1(4): 359-371.
(110) P Brundin, JY Li, JL Holton, O Lindvall and T Revesz (2008). Research in motion: the enigma of Parkinson's disease pathology spread. *Nat. Rev. Neurosci*. 9: 741–745.
(111) C Hansen, E Angot, AL Bergstrom, JA Steiner, L Pieri, G Paul, TF Outeiro, R Melki, P Kallunki, K Fog, JY Li and P Brundin (2011). Alpha-Synuclein propagates from mouse brain to grafted dopaminergic neurons and seeds aggregation in cultured human cells. *J. Clin. Invest*. 121: 715–725.
(112) JH Kordower, Y Chu, RA Hauser, TB Freeman and CW Olanow (2008). Lewy body-like pathology in long-term embryonic nigral transplants in Parkinson's disease. *Nat. Med*. 14: 504–506.
(113) JH Kordower, HB Dodiya, AM Kordower, B Terpstra, K Paumier, L Madhavan, C Sortwell, K Steece-Collier and TJ Collier (2011). Transfer of host-derived alpha synuclein to grafted dopaminergic neurons in rat. *Neurobiol. Dis*. 43: 552–557.
(114) JY Li, E Englund, JL Holton, D Soulet, P Hagell, AJ Lees, T Lashley, NP Quinn, S Rehncrona, A Bjorklund, H Widner, T Revesz, O Lindvall and P Brundin (2008). Lewy bodies in grafted neurons in subjects with Parkinson's disease suggest host-to-graft disease propagation. *Nat. Med*. 14: 501–503.
(115) Z Kurowska, E Englund, H Widnerd, O Lindvalle, JY Lia and P Brundin (2011). Signs of degeneration in 12–22-year old grafts of mesencephalic dopamine neurons in patients with Parkinson's disease. *J. Park. Dis*. 1: 83–92.
(116) CML Tomé, T Tyson, NL Rey, S Grathwohl, M Britschgi and P Brundin (2012). Inflammation and α-synuclein´s prion-like behavior in Parkinson´s disease - Is there a link? *Mol. Neurobiol*. 47(2): 561-574.
(117) H Lee, S Patel and S Lee (2005). Intravesicular localization and exocytosis of α-Synuclein and its aggregates. *The Journal of Neuroscience.* 25(25): 6016-6024.
(118) JA Steiner, E Angot and P Brundin (2011). A deadly spread: cellular mechanisms of alpha-synuclein transfer. *Cell and death differentiation*. 18: 1425-1433.
(119) Z Martinez, M Zhu, S Han and AL Fink (2007). GM1 specifically interacts with α-synuclein and inhibits fibrillation. *Biochemistry*. 46: 1868–1877.
(120) L Saavedra, A Mohamed, V Ma, S Kar and EP de Chaves (2007). Internalization of beta-amyloid peptide by primary neurons in the absence of apolipoprotein E. *J. Biol. Chem*. 282: 35722–35732.
(121) JY Park *et al.* (2009). On the mechanism of internalization of α-synuclein into microglia: roles of ganglioside GM1 and lipid raft. *J. Neurochem*. 110 : 400–411.
(122) E Emmanouilidou, K Melachroinou, T Roumeliotis, SD Garbis, M Ntzouni, LH Margaritis, L Stefanis, and K Vekrellis (2010). Cell-produced α-synuclein is

secreted in a calcium-dependent manner by exosomes and impacts neuronal survival. *J. Neurosci*. 30: 6838–6851.
(123) CJ Dunning, JR Reyes, JA Steiner and P Brundin (2012). Can Parkinson´s disease pathology be propagated from one neuron to another? *Progress in Neurrobiology*. 97: 205-219.
(124) SA Bellingham, BB Guo, BM Coleman and AF Hill (2012). Exosomes: vehicles for the transfer of toxic proteins associated with neurodegenerative diseases? *Front Physiol*. 3: 124.
(125) KM Danzer, LR Kranich, WP Ruf, O Cagsal-Getkin, AR Winslow, L Zhu, CR Vanderburg and PJ Mclean (2012). Exossomal cell-to-cell transmission of α-synuclein oligomers. *Mol. Neurodegener.* 7: 42.
(126) C Galvagnion, JWP Brown, MM Ouberai, P Flagmeier, M Vendruscolo, AK Buell, E Sparr and CM Dobson (2016). Chemical properties of lipids strongly affect the kinetics of the membrane-induced aggregation of α-synuclein. *PNAS* USA 113(26): 7065-7070.
(127) M Stöckl, P Fischer, E Wanker and A Harmann (2008). α-Synuclein selectively binds to anionic phospholipids embedded in liquid-disordered domains. *J. Mol. Biol.* 375: 1394-1404.
(128) E Jo, J McLaurin, CM Yip, P St. George-Hyslop and PE Fraser (2000). α-Synuclein membrane interactions and lipid specificity. *J. Biol. Chem.* 275(44): 34328-34.
(129) DL Fortin, MD Troyer, K Nakamura, S Kubo, MD Anthony and RH Edwards (2004). Lipid rafts mediate the synaptic localization of α-synuclein. *J. Neurosci.* 24: 6715-6723.
(130) JY Park, KS Kim, SB Lee, JS Ryu, KC Chung, YK Choo, I Jou, J Kim and SM Park (2009). On the mechanism of internalization of α-synuclein into microglia: roles of ganglioside GM1 and lipid raft. *J. Neurochem.* 110: 400-411.
(131) J Fantini and N Yahi (2011). Molecular basis for the glycosphingolipid-binding specificity of α-synuclein: key role of tyrosine 39 in membrane insertion. *J. Mol. Biol.* 408: 654-669.
(132) D Snead and D Eliezer (2014). α-Synuclein function and dysfunction on cellular membranes. *Exp. Neurobiol.* 23(4): 292-313.
(133) J Kiskis, I Horvath, P Wittung-Stafshede and S Rocha (2017). Unraveling amyloid formation paths of Parkinson´s disease protein α-synuclein triggered by anionic vesicles. *QRB-Discovery* 50,e3: 1-9.
(134) E Hellstrand, M Grey, M Ainalem, J Ankner, T Forsyth, G Fragneto, M Haertlein, M Dauvergne, H Nilsson, P Brundin, S Linse, T Nylander and E Sparr. (2013). Adsorption of α-synuclein to supported lipid bilayers - positioning and role of electrostatics. *ACS Chem Neurosci*. 4(10): 1339-1351.
(135) H Zhao, A Jutila, T Nurminen, SA Wickström, J Keski-Oja and PKJ Kinnunen (2005). Binding of Endostatin to phosphatidlyserine-containing membranes and formation of amyloid-like fibers. *Biochemistry*. 44: 2857-2863.

(136) S Chia, P Flagmeier, J Habchi, V Lattanzi, S Linse, CM Dobson, TPJ Knowles and M Vendruscolo (2017). Monomeric and fibrillar α-synuclein exert opposite effects on the catalytic cycle that promotes the proliferation of Aβ42 aggregates. *PNAS*. 114(30): 8005-8010.
(137) D Marsh (2013). Handbook of lipid bilayers. *CRC Press,* 2nd Edition 2013.

Acknowledgements

Emma and Sara..
Words will never come close to how thankful I am. But lacking the words, Thank you! ☺ I know for a fact that I'm the luckiest PhD student of all time, as I have had 2 always present supervisors that one can only wish for.

Emma, thank you for being my supervisor. I will never forget meeting you for the first time at the ECIS conference in Malmö. Right then and there I knew that everything would work out just fine. Thank you for all the guidance, teaching, support, help but most importantly always making me feel at home.

Sara, thank you for being my supervisor. I will never forget how you took the time to teach me step by step how to purify alpha-synuclein in my first week. Not something many supervisors would take the time to do. Right there and then I also knew everything would be just fine. Thank you for all the guidance, teaching, support, help but most importantly always making me feel at home.

Emma and Sara, thank you for all the trust, kindness and friendship these past years. My home, wherever I may end up next, will always be open to you and your family.

Björn Lindman.. Who knew that a half-semester course in Colloidal Chemistry in Coimbra would introduce me to my scientific mentor. I really don't have the words to express my gratitude, respect and admiration. I just hope to see you often!

Rui Brito, Filipe Antunes, Fafe e todos os elementos do grupo Colling, um obrigado especial por me terem abrigado e aturado no vosso espaço! Com grande orgulho digo que pretenço à família Colling. Filipe, obrigado por tudo. Nunca irei esquecer o teu apoio e a tua confiança, algo que só um verdadeiro amigo é capaz. Tirar a carta de mota contigo foi sem dúvida uma experiência, bem rápida! Ahahah

Members of the "Biochemi side", it has been truly awesome! Thanks for making such a nice environment. **Asharr**, thanks for the great company. **Birgitta**, thanks for all the help and guidance in the lab. **Chris Dunning, Marie Grey and Erik Hellstrand** thank you for introducing me to everything and everyone in the lab. It is pretty easy to start on a project with people like you. Thanks Marie for letting

me use your cryo-image as the back cover of the thesis. ☺ **Cecilia**, thanks for all your contributions to my project. **Elodie**, obrigado por tudo! **Kalyani**, thanks for all the support. We had a great time in Cambridge! **Karin**, thanks for the nice chats and company. **Katia**, thanks for all the help and the endless supply of alpha-synuclein! **Martin and Celia**, thanks for everything, I really learnt a lot working with you. **Mattias**, awesome times in Stockholm. Thanks for everything buddy. **Olof**, thanks for the nice chats and BBQs. **Risto**, thanks for being who you are buddy. It was super nice to spend time with you, either watching games, drinking beers or playing soccer. See you soon when you come to visit. **Rebecca**, thanks for the super nice chats and company. **Stefan and Tinna**, thanks for all the help, support and super nice times watching Iceland. **Tommy**, thank you for helping me with the disc centrifuge and other important discussions. I hope to see you soon in Portugal! **Tanja**, thanks for all the support and doing Colloidal domain with me. **Thom**, thanks for always being patient and helping me deal with the plate reader! **Xiaoting and Weimin**, thanks for the nice chats and hot pot! **Uli** thanks buddy for all the collaborative work, BBQs and champion league games. **Veronica**, thanks for the craziness, company and super nice chats. **Wen**, thanks for all the nice chats and company during our long working hours.

Tuomas, Alex, Céline, Georg, Laurie and Clemens, thanks for the super nice collaborative work and discussions. Also, thank you for receiving me so well in Cambridge and allowing me to work and learn from you.

To all members of the "Phys-Chemi side", it has been super fun! Thanks to all my cool office mates for putting up with me: **Jenny, Jessie, Julien, Kasia, Sofi and Ilaria**. To previous members, thanks for creating a welcoming and great environment, it was super nice to start working belonging to such an awesome group: **Aleksandra, Charlotte, Emelie, Guilherme, Jon, Mariana, Marta, Solmaz, Sanna, Saskia and Stefanie**. To all the present members, **Axel, Antara, Dóra, Felix, Jasper, Johan, Luigi, Linda, Marta, Maxime, Polina and Vicky** thanks for all the good times, after works, lunches, dinners, beers, parties.. It wouldn't have been the same without you! ☺ To the Portuguese clan, **Bruno, Hugo, João Martins, Tiago F., Tiago M.**, **Diogo**, **Tiago C**., what to say, thanks for the good times and viva "As loiras!". **Carlos Urey**, thanks for the nice chats and it was awesome playing on your team. **Göran**, thanks for all the NMR knowledge. **Jon P**., thanks for super nice times in Uppsala and for all the collaborative work. **Dat**, thanks for being awesome buddy and all the help! **Enamul**, thanks for the super nice discussions and collaborative work. **Tommy G**., thanks for all the friendship. Super proud of our work together! **Marc**, thanks for all the support. **Maria V**., "espanholita" thanks for all the help with QCM-D and for being super nice! **Max**, dude we will always have "donuts" and "electron clouds!" ahahah. **Monika and Kira**, I hope I wasn't a horrible "supervisor" ☺,

thanks for all the energy and good times. **Thiago**, “tuga-emprestado”, eheh. Cara, obrigado por tudo amigão, mesmo.. Espero uma visita tua em breve.

To all the Phys. Chem. Professors, **Anna, Daniel, Häkan, Karin, Lennart, Mikael, Olle, Peter Jönsson, Tommy N., Ulf and Viveka** thanks for creating the perfect environment to learn and preform science. Thank you for all the support and help given to me during my PhD. **Maria S. and Helena**, thanks for everything! And that doesn’t even come close to how important you have been in my PhD. **Anna and Gunnel**, thank you for being so friendly during the cryo-TEM sessions. Thank you **Paula** for all the help printing the thesis.

To all my soccer buddies from **ESN FC, Pressbeerån FC and BMC FC** it was awesome!

I would also like to thank **Multipark and The Royal Swedish Academy of Sciences** for the financial support given to me during my PhD.

To all my friends outside the lab, thanks for all the support given to me these past years. **Núcleo forte, my “chops” and all my family/friends**. Friends for life! Professores **Paula Veríssimo**, **Carrilho** e **Zé Manel** obrigado por terem sido inspiradores!

“If it were easy, everyone would do it”. That´s a phrase a pretty much heard every time I spoke with my parents during my PhD thesis. It kinda of makes sense now.. I would really like to thank my **Mom and Dad**, who are truly my best friends and have supported me in everything since before I can remember. Obrigado por serem exatamente quem são! **Família Gaspar e Soares** obrigado por tudo! **Tia Fátima**, **Tio Carlos**, **Becca**, **Nicky**, **Tio Paulo** e **Avó Lurdes** um especial obrigado! To my wife (still haven gotten use to saying that.. eheheh), **Cristina**, thanks for being patient, supportive and putting your career on hold and moving to Sweden for us. A tua presença e apoio foram tudo! Last, but definitely the most important person in my life, my son, **Isaac**! Thanks for keeping me up all night, it increased my working hours! ☺ Thanks for being simply perfect. This thesis is dedicated to you, and the rest of the family, in particular to my **Avó Bassilissa**.

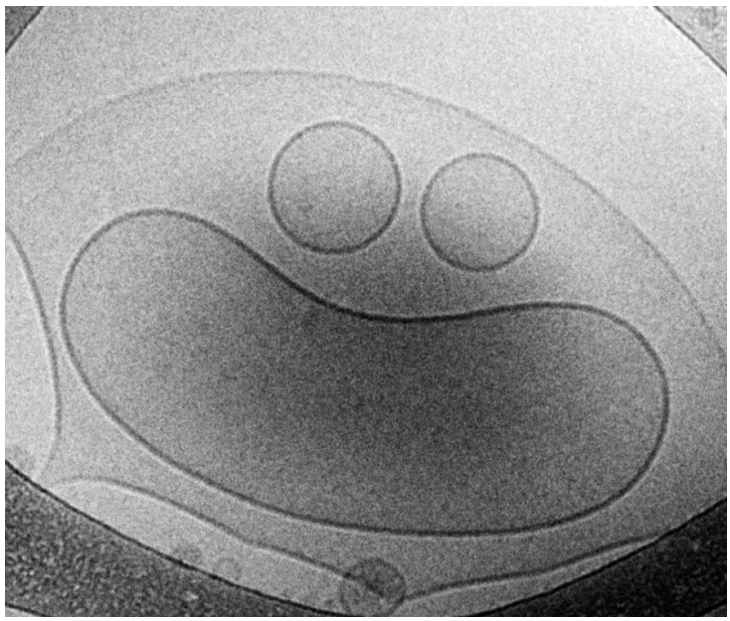

Printed by Media-Tryck, Lund 2018 NORDIC SWAN ECOLABEL 3041 0903

LUND UNIVERSITY

ISBN: 978-91-7422-599-0

Physical Chemistry
Faculty of Science
Lund University

9 789174 225990